FINITE ELEMENT ANALYSIS OF DYNAMIC STABILITY OF CYLINDRICAL RODS SUBJECTED TO PARALLEL FLOW

By
SHRAWAN KUMAR URMALIA

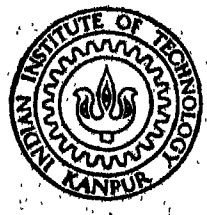

DEPARTMENT OF MECHANICAL ENGINEERING
INDIAN INSTITUTE OF TECHNOLOGY, KANPUR
JUNE, 1978

ME-1978-M-URM-FIN

MOST SINCERELY DEDICATED TO THE WOMEN
WHO MATTERED IN MY LIFE -

MY NANIMA
MY MOTHER
SISTER MANORAMA
AND
SHASHI, MY WIFE

CERTIFICATE

Certified that the work entitled "Finite Element Analysis of Dynamic Stability of Cylindrical Rods Subjected to Parallel Flow", which is being submitted by Mr. Shrawan Kumar Urmalia in partial fulfilment of the award of the degree of MASTER OF TECHNOLOGY, has been carried out under my supervision and has not been submitted elsewhere for the award of a degree.

Bhupinder Pal Singh

Bhupinder Pal Singh
Assistant Professor
Department of Mech. Engineering
Indian Institute of Technology
KANPUR

ACKNOWLEDGEMENTS

It gives me great pleasure to express my heartfelt gratitude towards Dr. Bhupinder Pal Singh for his constant encouragement, timely guidance, invaluable comments and fruitful criticism throughout the course of this work.

I acknowledge with thanks the invaluable cooperation and timely help received from Messrs. J.K. Deb, Vishwanath Bajpai, R.K. Singh, I.S. Singh, V.K. Nair and H.K. Kanodia and I owe my thanks to all of my friends, past and present, who helped me one way or the other.

I must express my appreciation to Mr. R.P. Suri, Mr. N.P. Roberts and Mr. Y.D.S. Arya of the Computer Centre, IIT/Kanpur for their useful help during the computational work.

I am thankful to Mr. D.K. Misra for his timely help in tracing the figures.

Last but not the least, to Mr. D.P. Saini go my thanks for his patient and accurate typing.

JUNE, 1978 S.K. URMALIA

CONTENTS

LIST OF FIGURES

Page

LIST OF TABLES

NOMENCLATURE

A : Cross-sectional area of rod.

$[c]^e$: Damping matrix for the element.

$[C]$: Assembled damping matrix after applying boundary conditions.

$[C]_{BB}$: Assembled damping matrix before applying boundary conditions.

C_b : Base drag coefficient.

C_D : Coefficient of viscous damping

C_f : Skin friction drag coefficient.

c_b : Equal to $(4/\pi)\, C_b$.

c_d : Equal to $C_D L(M/EI)^{1/2}$.

c_f : Equal to $(4/\pi)\, C_f$.

C_m : Coefficient of virtual mass.

D : Diameter of rod.

$[D]$: Dynamical matrix.

E : Modulus of elasticity of the rod material.

EI : Flexural rigidity of the rod.

F_A : Inviscid hydrodynamic force on rod, per unit length.

F_D : Viscous damping force on rod, per unit length.

F_N : Normal viscous force on rod, per unit length.

F_L : Longitudinal viscous force on rod, per unit length.

F_{px}, F_{py} : Steady state pressure forces on rod, per unit length.

F_x, F_y : Total forces in x- and y-directions.

f : Number of degrees of freedom assigned to the element.

f_c : Slenderness coefficient for hydrodynamic forces at a free end.

g : Acceleration due to gravity.

h : Length of the typical finite element.

I : Moment of Inertia of the rod.

$Im(\omega)$: Imaginary part of the eigenvalue.

K_{dO}, K_{dL} : Displacement spring constants at $x = 0$ and $x = L$, respectively.

K_{tO}, K_{tL} : Rotational spring constants, at $x = 0$ and $x = L$, respectively.

$[k]^{(e)}$: Stiffness matrix for the element.

$[K]$: Assembled stiffness matrix after applying boundary conditions.

$[K]_{BB}$: Assembled stiffness matrix before applying boundary conditions.

$[\bar{K}]$: Stiffness matrix for the dynamical matrix.

l : Length of the tapered portion of a cantilevered rod with tapered free end.

L : Length of rod.

m : Number of elements.

$m + 1$: Number of nodes.

m_f : Virtual mass of rod per unit length.

m_r : Mass of rod per unit length.

$[m]^{(e)}$: Mass matrix for the element.

$[M]$: Assembled mass matrix after applying boundary conditions.

$[M]_{BB}$: Assembled mass matrix before applying boundary conditions.

$[\bar{M}]$: Mass matrix for the dynamical matrix.

$|M|$: Moment on a cross-section of the rod.

$N_i(x)$: Interpolation functions.

$|L|$: Interpolation matrixx.

$|N'|$: First derivative of N with respect to x.

$|N''|$: Second derivative of N with respect to x.

n : Represents order of the matrix.

p : Steady-state pressure of the fluid.

$\overline{pA}$: pA at $x = L/2$.

p_b : Base pressure.

Q : Shear force on a cross-section of the rod.

$Q(t)$: Forcing function. $\left\{ \begin{matrix} \{\dot{y}(t)\} \\ \{y(t)\} \end{matrix} \right\}$

$\{q(t)\}$: Equal to

$Re(\omega)$: Real part of the eigenvalue.

t : Time.

T : Tension on a cross-section of the rod.

$\bar{T}$: Externally applied, uniform tension.

u : Dimensionless fluid velocity.

u_b : Critical dimensionless flow velocity for buckling.

u_{c0} : Critical dimensionless flow velocity for flutter.

u_L : Change in length of the rod.

v : Resultant relative velocity between the rod and the fluid.

V : Mean flow velocity of the fluid.

V_x : Axial component of fluid velocity V.

V_y : Transverse component of fluid velocity V.

W : Equal to $F_L + (m_r - m_f) g$

x : Axial co-ordinate of the rod.

x_e : Defined by Eqn. (6-4).

x_p : Axial co-ordinate of the element.

X : Coefficient of $(\partial y / \partial t)$.

$\{ Y(t) \}$: Equal to $\begin{Bmatrix} \{0\} \\ \{ Q(t) \} \end{Bmatrix}$.

y : Lateral displacement of the rod.

$y_i(t)$: Typical element of the nodal displacement matrix $\{ y \}^{ne}$.

y_p, y_q : Lateral displacements at nodes p and q, respectively.

$\{ y^n \}$: Nodal displacement matrix for the rod.

$\{ \dot{y}^n \}$: Nodal velocity matrix for the rod.

$\{\ddot{y}\}^n$: Nodal acceleration matrix for the rod.

$\{y\}^{ne}$: Nodal displacement matrix for the finite element.

$\{\dot{y}\}^{ne}$: Nodal velocity matrix for the finite element.

$\{\ddot{y}\}^{ne}$: Nodal acceleration matrix for the finite element.

Z : Coefficient of $(\partial^2 y/\partial x^2)$.

GREEK SYMBOIS

α : Dimensionless internal damping coefficient.

α_d : Dimensionless displacement spring factor.

α_t : Dimensionless rotational spring factor.

β : Dimensionless mass.

γ : Dimensionless gravity parameter.

Γ : Dimensionless uniform tension.

δ : Equal to 0 or 1 accordingly as the cylinder is free or not to slide axially at $x = L$.

ε : Equal to L/D.

η : Dimensionless pressure parameter.

$\bar{\theta}$: Angle of inclination of rod to flow.

θ_p , θ_q : Slopes $\partial y/\partial x$, at the nodes p and q, respectively.

λ : Eigenvalues.

μ : Internal damping coefficient.

ν : Poisson's ratio.

ξ_1 : Length co-ordinate $1 - \frac{x}{h}$,

ξ_2 : Length co-ordinate $= \frac{x}{h}$.

ρ_f : Fluid density.

$\{ \phi \}$: Vector consisting of 2n constant elements.

ω_I , ω_R : Imaginary and real parts of complex natural frequency, respectively.

SYMBOLS FOR MATRICES

$\{ \}$: Column matrix or column vector.

$\lfloor \rfloor$: Row matrix or row vector.

$[ ]$: Square matrix.

ABSTRACT

This work deals with the dynamical stability of flexible cylindrical rods subjected to external parallel, uniform and steady flow. A general finite element model is presented for isolated rods considering old and new formulations. System matrices are obtained using finite element based Galerkin's method and natural boundary conditions have been considered explicitly in these matrices along with the geometric boundary conditions. The results obtained in the form of complex eigenvalues for old and new formulations have been compared, wherever possible, with the available results through Argand diagrams, and discussed. Good agreement is found for pinned-pinned and cantilever (with tapered free end) rods except in the ill-conditioned range, where even available results can not be relied upon. Results for clamped-clamped rods for old formulation are corrected. New results are shown for clamped-clamped rods for new formulation.

A generalized computer programme is developed to form the dynamical matrix, which gives complex eigenvalues by calling a library subroutine ZINDIA. An important feature of this programme is its flexibility. It can accommodate all the boundary conditions by making few changes in the input cards.

CHAPTER I

INTRODUCTION

1.1 INTRODUCTION TO FLOW-INDUCED VIBRATION PROBLEM

The response of a structure, when subjected to an external flow and/or containing a flowing fluid, is of considerable practical importance and is encountered in various engineering system components, such as nuclear fuel bundles (rods) and heat exchanger tubes etc. The dynamic behavior of such structures is quite complex and it has been a matter of interest for many dynamicists for last two decades. This type of problem, where the flow of the fluid, external and/or internal, is responsible for the vibration of the structures, is termed as "Flow-Induced Vibration Problem". In reference to the orientation of the fluid flow with respect to the axis of the structure, the flow induced vibration problem may be classified as follows:

1. Parallel flow, i.e., fluid is flowing parallel to the axis of the rod. It is further subdivided as:
   (a) Internal flow,
   (b) External flow, and
   (c) Internal and External flow.
2. Cross flow, i.e., fluid is flowing perpendicular to the axis of the rod.

Present work involves the study of dynamic stability of a single rod subjected to parallel external flow by the finite element method.

Fluid flowing past a system is a source of energy, which is imparted to the system components. This energy is responsible for the vibration of the system components which may cause instability in the system. This instability, ultimately, may cause the system damage.

At small flow velocities, instability usually does not occur. As the flow velocity increases, the structure becomes unstable at a certain velocity. This velocity is called critical velocity. This instability may be of buckling type and/or oscillatory type. These instabilities are pronounced enough to cause failure of the system components, and hence need to be investigated so that the system can be designed to withstand the flow-induced vibrations.

Analysis of the flow-induced vibration problems need the response, i.e., the actual motion of the structure, and the stability of the structure, i.e., to know, how sensitive the structure is for the changes made in the system parameters involved therein. The stability analysis often supplies sufficient information to consider the vibration problem as solved. Moreover this analysis is comparatively simpler. The response analysis requires the complete knowledge of the fluid dynamics, i.e., damping mechanism and flow originated excitation which may be due to unsteady pressure field or pulsations in the flow rate.

1.2 PREVIOUS WORK ON THE DYNAMICS OF RODS SUBJECTED TO PARALLEL EXTERNAL FLOW

It was Burgreen et. al [2] who first demonstrated the phenomenon of rod vibration caused by the parallel flow of a fluid past a cylindrical rod in the year 1958, while studying the heat transfer of water flowing across a bundle of rods in a nuclear reactor core. He observed the oscillations to occur at all flow velocities. Also the oscillations were found to be relatively constant throughout the whole range of velocities which led him to believe that the vibration was of self-excited type. He developed an empirical expression for maximum amplitude of vibration by dimensional analysis of differential equation of motion assuming excitation force to be proportional to the dynamic pressure ($\frac{1}{2} \rho V^2$) of the fluid. This was followed by several experimental studies [12, 15, 21, 22] , with different excitation forces, wherein the main aim was to study the character of the vibrations and obtain an empirical expression for maximum amplitude of vibration which can be used to solve mechanical design problems in reactors and heat exchangers.

In these experimental studies, various researchers assumed different forcing functions and obtained empirical expressions for maximum amplitude of vibration. Most of them [3] selected turbulent-boundary layer pressure fluctuation as the forcing function.

The first analytical and experimental treatment of the problem was presented by Paidoussis [14] in 1966. His mathematical

model was based on Bernoulli-Euler beam theory to describe the flexural motions of the cylindrical body, slender body theory for the coupled inviscid hydrodynamic forces, and fairly reasonable relationships for the corresponding viscous forces. He considered three boundary conditions; namely pinned-pinned ends, clamped-clamped ends and clamped-free ends with tapered, streamlined downstream end and showed that small flow velocities damp the free motion of the system but high flow velocities induce buckling and oscillatory hydroelastic instabilities. He showed that flutter instabilities are caused by lateral frictional forces, and in the absence of hydrodynamic-drag effects only buckling instability is possible. Externally applied tension was observed to stabilize the system while compression destabilized it.

Paidoussis [16] extended his previous study of the dynamics of flexible cylinders in axial flow and presented a general theory to account for the small, free, lateral motions of a flexible, slender, cylinderical body with tapered ends, totally submerged in liquid and towed at steady speed V. For particular shapes of the ends and length of tow-rope, he showed that the body may be subjected to oscillatory and non-oscillatory instabilities for $V > 0$; at small V, these instabilities correspond to those of a rigid body. He also showed that at higher V, the system generally regains stability in the above modes, but may be subjected to higher-mode, flexural oscillatory instabilities. The effect of a number of dimensionless parameter on

stability were calculated to obtain the critical conditions of stability. It was shown that optimum stability is achieved with a streamlined nose, a blunt tail and a short tow-rope.

In 1973, Paidoussis [17] extended the theory by including material damping, gravity, pressure forces and fluid damping force, and also applied the theory to cylinders in confined flows. In this work frictional forces were taken into account correctly. He showed that small flow velocities damp free motions, but at sufficiently high velocities hydroelastic instabilities occur. Pinned-pinned cylinders are subjected to buckling in their first mode, and then at higher flow velocities in their second mode; at slightly higher flow velocities coupled-mode flutter was observed. Critical velocities for the cylinder in a closely spaced cluster were much lower than those for an isolated one. Cantilever cylinders, on the other hand, were subjected to buckling in their first mode and to flutter in their higher modes. He carried out the calculations for cantilevers for high velocities. These enabled him to observe that the loss of stability in the second mode is preceded by regaining of stability in the first mode; then in the similar manner second mode regains stability at a slightly higher velocity than is necessary for the onset of third mode flutter. He also discussed the case of cylinders in axial flow subjected to an arbitrary force field.

Recently in 1975, Paidoussis 20 analysed the stability of a tind

Recently in 1975, Paidoussis [20] analysed the stability of slender cylinders with pinned-pinned ends and clamped-free ends, subjected to axial flow with harmonically perturbed velocity. He showed the possibility of instabilities for certain ranges of frequencies and amplitudes of the perturbations. The parameters which destabilize the system in steady flow, make the parametric instability regions wider. In case of simply-supported cylinders parametric instabilities occur over specific ranges of flow velocities. In the case of cantilever cylinders the instabilities were found to occur in some of the modes of the system and the regions of these instabilities in strutt diagrams were quite complex. Moreover, the regions of instability in strutt diagrams became wider as the system approached the point of instability in steady flow.

1.3 PRESENT WORK

In the present work the flow-induced vibration problem, in which vibration of the rods is caused by external parallel flow, has been solved by the finite element method and the dynamical behavior of the rods with different boundary conditions has been studied. Old formulation, Paidoussis [14], and, the new formulation, Paidoussis [17], both, have been considered for studying the dynamics of rods with pinned-pinned ends, clamped-clamped ends and clamped-tapered free ends. The results obtained in the present work have been compared, wherever possible, with the available results for

old and new formulations. Also, the effect of various non-dimensional parameters on the stability of the erods has been studied and compared with the available results.

In the second chapter the equations of motion are obtained in the matrix form by the finite element analysis using Galerkin's method. The stiffness, damping and mass matrices for a typical finite element are obtained. After assembling these matrices for the whole domain, natural boundary conditions (as a result of finite element based Galerkin's method) and geometric boundary conditions are introduced. Finally, the system dynamical matrix is obtained by arranging these matrices. Method of solution is also discussed in this chapter.

Complex eigenvalues of the dynamical matrix are computed using a library subroutine for various boundary conditions. The various dimensionless parameters, whose effects studied on the stability of pinned-pinned rods are :

(a) effect of dimensionless mass (β)

(b) effect of external tension (Γ)

(c) effect of internal damping (α)

(d) effect of gravity (γ)

All the results obtained are illustrated and discussed in the third chapter. Furthermore, mechanism of instability is also discussed briefly in this chapter.

Chapter four contains the conclusions on the basis of the results obtained in the present work.

Further, in Appendix A, various fluid forces resulting from the fluid flow have been discussed in detail. Also governing equation for small lateral motions for an isolated rod has been derived.

Appendix B deals with the old formulation of the problem and its finite element analysis. The difference between old and new formulations has been discussed in brief. Appendix C gives the boundary conditions for a cantilever rod with tapered free end.

Lastly, the computer programme has been introduced in Appendix D whose detailed listing is given in Appendix E.

CHAPTER II

FORMULATION OF PROBIEM AND COMPUTATIONAL APPROACH

In the present chapter the fifth order differential equation governing the transverse motion of a rod in an infinite fluid flowing at a velocity V is converted into simultaneous differential equations by finite element method using Galerkin's method. Further, these equations are rearranged to form standard eigenvalue problem to obtain complex eigenvalues.

2.1 FINITE ELEMENT ANALYSIS :

The governing equation of motion for the small transverse vibration of a flexible slender rod of circular cross-section immersed in an infinite fluid flowing with a uniform velocity V can be written as, Paidoussis [17],

$$\mu I \frac{\partial^5 y}{\partial x^4 \partial t} + EI \frac{\partial^4 y}{\partial x^4} + C_m m_f \frac{\partial^2 y}{\partial t^2} + 2 C_m m_f V \frac{\partial^2 y}{\partial x \partial t}$$

$$+ C_m m_f V^2 \frac{\partial^2 y}{\partial x^2} - \{\delta [\bar{T} + (1-2\nu)(\bar{pA})] +$$

$$+ [\frac{1}{2} \rho_f D V^2 C_f + (m_r - m_f) g] [(1 - \frac{1}{2}\delta) L - x]$$

$$+ \frac{1}{2} \rho_f D^2 V^2 C_b (1 - \delta)\} \frac{\partial^2 y}{\partial x^2} + \frac{1}{2} \rho_f D V C_f \frac{\partial y}{\partial t} + \frac{1}{2} \rho_f D V^2 C_f \frac{\partial y}{\partial x}$$

$$+ \frac{1}{2} \rho_f D C_D \frac{\partial y}{\partial t} + (m_r - m_f) g \frac{\partial y}{\partial x} + m_r \frac{\partial^2 y}{\partial t^2} = 0, \qquad (2.1)$$

with the boundary conditions as

$$EI\frac{\partial^3 y}{\partial x^3} + \mu I\frac{\partial^4 y}{\partial x^3\,\partial t} - \left(\overline{T} + (1-2\nu)\left(\overline{pA}\right)\right)\frac{\partial y}{\partial x}$$

$$+ K_{d0}\, y = 0 \quad \text{or } y = 0 \text{ at } x = 0,$$

$$EI\frac{\partial^2 y}{\partial x^2} + \mu I\frac{\partial^3 y}{\partial x^2\,\partial t} - K_{t0}\frac{\partial y}{\partial x} = 0 \quad \text{or } \frac{\partial y}{\partial x} = 0 \text{ at } x = 0,$$

$$EI\frac{\partial^3 y}{\partial x^3} + \mu I\frac{\partial^4 y}{\partial x^3\,\partial t} - \left(\overline{T} + (1-2\nu)\left(\overline{pA}\right)\right)\frac{\partial y}{\partial x}$$

$$- K_{dL}\, y = 0 \quad \text{or } y = 0 \text{ at } x = L,$$

$$EI\frac{\partial^2 y}{\partial x^2} + \mu I\frac{\partial^3 y}{\partial x^2\,\partial t} + K_{tL}\frac{\partial y}{\partial x} = 0 \quad \text{or } \frac{\partial y}{\partial x} = 0 \text{ at } x = L, \qquad \ldots\ldots \qquad (2.2)$$

where Z and W are given by Eqns. (2.3) and (2.4), respectively, and

μ = internal damping coefficient representing a Kelvin-Voigt type of damping in the material of the rod.

EI = flexural rigidity of the rod.

C_m = coefficient of virtual mass.

m_f = virtual mass of rod per unit length.

m_r = mass of rod per unit length.

V = mean flow velocity of the fluid.

δ = equal to 0 or 1 accordingly as the rod is free or not to slide axially at $x = L$.

$\overline{T}$ = externally applied, uniform tension.

ν = Poisson's ratio.

p = steady-state pressure of the fluid.

A = cross-sectional area of rod.

$\overline{pA}$ = pA at $x = \frac{L}{2}$.

ρ_f = density of the fluid.

D = diameter of rod.

C_f = skin friction drag coefficient.

C_D = coefficient of viscous damping.

C_b = base drag coefficient.

L = length of rod.

x = axial co-ordinate.

t = time.

y = lateral displacement of rod.

K_{dO}; K_{dL} = displacement spring constants at $x = 0$ and $x = L$, respectively.

K_{tO}, K_{tL} = rotational spring constants at $x = 0$ and $x = L$, respectively.

For the sake of simplicity, various terms in Eqn. (2.1) associated with $\frac{\partial^2 y}{\partial x^2}$, $\frac{\partial y}{\partial x}$ and $\frac{\partial y}{\partial t}$ are put in the following manner :

$$Z = (C_m m_f V^2 - \{\delta [\overline{T} + (1 - 2\nu)(\overline{pA})] + [\tfrac{1}{2} \rho_f D V^2 C_f + (m_r - m_f)g]$$

$$[(1 - \tfrac{1}{2}\delta) L] + [\tfrac{1}{2} \rho_f D^2 V^2 C_b (1 - \delta)]\}), \quad (2.3)$$

$$\int_0^h N_i \left[(m_r + C_m m_f) \frac{\partial^2 y^{(e)}}{\partial t^2} + \mu I \frac{\partial^5 y^{(e)}}{\partial x^4 \partial t} + 2 C_m m_f V \frac{\partial^2 y^{(e)}}{\partial x \partial t} \right.$$

$$\left. + X \frac{\partial y^{(e)}}{\partial t} + EI \frac{\partial^4 y^{(e)}}{\partial x^4} + Z \frac{\partial^2 y^{(e)}}{\partial x^2} + W \left((x_p + x) \frac{\partial^2 y^{(e)}}{\partial x^2} + \frac{\partial y^{(e)}}{\partial x} \right) \right] dx = 0,$$

$$i = 1, 2, \ldots\ldots, f. \qquad (2.8)$$

Now, the above equation is integrated by parts to introduce the natural boundary conditions and reduce the order of derivatives simultaneously.

Second term is integrated twice and it results,

$$\int_0^h N_i \, \mu I \frac{\partial^5 y^{(e)}}{\partial x^4 \partial t} dx = \left| N_i \, \mu I \frac{\partial^4 y^{(e)}}{\partial x^3 \partial t} \right|_0^h - \left| \frac{dN_i}{dx} \, \mu I \frac{\partial^3 y^{(e)}}{\partial x^2 \partial t} \right|_0^h$$

$$+ \int_0^h \frac{d^2 N_i}{dx^2} \, \mu I \frac{\partial^3 y^{(e)}}{\partial x^2 \partial t} dx . \qquad (2.9)$$

Third term, after integrated once, yields,

$$\int_0^h N_i \, 2 C_m m_f V \frac{\partial^2 y^{(e)}}{\partial x \partial t} dx = \left| N_i \, 2 C_m m_f V \frac{\partial y^{(e)}}{\partial t} \right|_0^h$$

$$- \int_0^h \frac{dN_i}{dx} \, 2 C_m m_f V \frac{\partial y^{(e)}}{\partial t} dx . \qquad (2.10)$$

Fifth term is also integrated twice and it gives,

$$\int_0^h N_i \, EI \frac{\partial^4 y^{(e)}}{\partial x^4} dx = \left| N_i \, EI \frac{\partial^3 y^{(e)}}{\partial x^3} \right|_0^h - \left| \frac{dN_i}{dx} \, EI \frac{\partial^2 y^{(e)}}{\partial x^2} \right|_0^h$$

$$+ \int_0^h \frac{d^2 N_i}{dx^2} EI \frac{\partial^2 y^{(e)}}{\partial x^2} dx . \qquad (2.11)$$

Sixth term reduces to,

$$\int_0^h N_i Z \frac{\partial^2 y^{(e)}}{\partial x^2} dx = \left| N_i Z \frac{\partial y^{(e)}}{\partial x} \right|_0^h - \int_0^h \frac{dN_i}{dx} Z \frac{\partial y^{(e)}}{\partial x} dx . \quad \ldots\ldots (2.12)$$

Seventh term turns out to be very interesting (two terms are combined) and its integration by parts gives,

$$\int_0^h N_i W((x_p + x) \frac{\partial^2 y^{(e)}}{\partial x^2} + \frac{\partial y^{(e)}}{\partial x}) dx = \left| N_i W (x_p + x) \frac{\partial y^{(e)}}{\partial x} \right|_0^h - \int_0^h \frac{dN_i}{dx} W (x_p + x) \frac{\partial y^{(e)}}{\partial x} dx . \quad (2.13)$$

Substituting Eqns. (2.9), (2.10), (2.11), (2.12) and (2.13) in Eqn. (2.8), it takes the following form,

$$\int_0^h \{[(m_r + C_m m_f) N_i \frac{\partial^2 y^{(e)}}{\partial t^2}] + [\mu I \frac{d^2 N_i}{dx^2} \frac{\partial^3 y^{(e)}}{\partial x^2 \partial t} - 2 C_m m_f V \frac{dN_i}{dx} \frac{\partial y^{(e)}}{\partial t} + X N_i \frac{\partial y^{(e)}}{\partial t}] + [EI \frac{d^2 N_i}{dx^2} \frac{\partial^2 y^{(e)}}{\partial x^2} - Z \frac{dN_i}{dx} \frac{\partial y^{(e)}}{\partial x} - W x_p \frac{dN_i}{dx} \frac{\partial y^{(e)}}{\partial x} - W x \frac{dN_i}{dx} \frac{\partial y^{(e)}}{\partial x}]\} dx + \left| N_i \mu I \frac{\partial^4 y^{(e)}}{\partial x^3 \partial t} \right|_0^h - \left| \frac{dN_i}{dx} \mu I \frac{\partial^3 y^{(e)}}{\partial x^2 \partial t} \right|_0^h + \left| N_i 2 C_m m_f V \frac{\partial y^{(e)}}{\partial t} \right|_0^h + \left| N_i EI \frac{\partial^3 y^{(e)}}{\partial x^3} \right|_0^h - \left| \frac{dN_i}{dx} EI \frac{\partial^2 y^{(e)}}{\partial x^2} \right|_0^h + \left| N_i Z \frac{\partial y^{(e)}}{\partial x} \right|_0^h + \left| N_i W (x_p + x) \frac{\partial y^{(e)}}{\partial x} \right|_0^h = 0 ,$$

$$i = 1,2,\ldots., f . \quad (2.14)$$

Again, to have the system matrices, Eqn. (2.7) is substituted into the above Eqn. (2.14) and rearranging, one gets for the element, e,

$$[m]^{(e)}\{\ddot{y}\}^{ne} + [c]^{(e)}\{\dot{y}\}^{ne} + [k]^{(e)}\{y\}^{ne} + \begin{Bmatrix} \left| N_1 \ \mu I \frac{\partial^4 y^{(e)}}{\partial x^3 \ t} \right|_0^h \\ \left| N_2 \mu I \frac{\partial^4 y^{(e)}}{\partial x^3 \ t} \right|_0^h \\ \vdots \\ \left| N_f \mu I \frac{\partial^4 y^{(e)}}{\partial x^3 \ t} \right|_0^h \end{Bmatrix}$$

$$- \begin{Bmatrix} \left| N_1' \ \mu I \frac{\partial^3 y^{(e)}}{\partial x^2 \ \partial t} \right|_0^h \\ \left| N_2' \ \mu I \frac{\partial^3 y^{(e)}}{\partial x^2 \ \partial t} \right|_0^h \\ \vdots \\ \left| N_f' \ \mu I \frac{\partial^3 y^{(e)}}{\partial x^2 \ \partial t} \right|_0^h \end{Bmatrix} + \begin{Bmatrix} \left| N_1 \ 2 C_m m_f V \frac{\partial y^{(e)}}{\partial t} \right|_0^h \\ \left| N_2 \ 2 C_m m_f V \frac{\partial y^{(e)}}{\partial t} \right|_0^h \\ \vdots \\ \left| N_f \ 2 C_m m_f V \frac{\partial y^{(e)}}{\partial t} \right|_0^h \end{Bmatrix}$$

$$+ \begin{Bmatrix} \left| N_1 \ EI \frac{\partial^3 y^{(e)}}{\partial x^3} \right|_0^h \\ \left| N_2 \ EI \frac{\partial^3 y^{(e)}}{\partial x^3} \right|_0^h \\ \vdots \\ \left| N_f \ EI \frac{\partial^3 y^{(e)}}{\partial x^3} \right|_0^h \end{Bmatrix} - \begin{Bmatrix} \left| N_1' \ EI \frac{\partial^2 y^{(e)}}{\partial x^2} \right|_0^h \\ \left| N_2' \ EI \frac{\partial^2 y^{(e)}}{\partial x^2} \right|_0^h \\ \vdots \\ \left| N_f' \ EI \frac{\partial^2 y^{(e)}}{\partial x^2} \right|_0^h \end{Bmatrix}$$

$$+\left\{\begin{array}{l} \left| N_1 \, Z \, \frac{\partial y^{(e)}}{\partial x} \right|_0^h \\ \left| N_2 \, Z \, \frac{\partial y^{(e)}}{\partial x} \right|_0^h \\ \vdots \\ \left| N_f \, Z \, \frac{\partial y^{(e)}}{\partial x} \right|_0^h \end{array}\right\} + \left\{\begin{array}{l} \left| N_1 \, W \, (x_p + x) \frac{\partial y^{(e)}}{\partial x} \right|_0^h \\ \left| N_2 \, W \, (x_p + x) \frac{\partial y^{(e)}}{\partial x} \right|_0^h \\ \vdots \\ \left| N_f \, W \, (x_p + x) \frac{\partial y^{(e)}}{\partial x} \right|_0^h \end{array}\right\} = \{0\} \quad (2.15)$$

where

$[m]^{(e)}$ = mass matrix for the element

$$= \int_0^h (m_r + C_m m_f) \{N\} \lfloor N \rfloor \, dx \quad (2.16)$$

$[c]^{(e)}$ = total damping matrix for the element

$$= [c1]^{(e)} + [c2]^{(e)} + [c3]^{(e)} \quad (2.17)$$

$[c1]^{(e)}$ = internal damping matrix for the element

$$= \int_0^h \mu I \{N''\} \lfloor N'' \rfloor \, dx \quad (2.18)$$

$[c2]^{(e)}$ = coriolic force damping matrix for the element

$$= - \int_0^h 2 C_m m_f V \{N'\} \lfloor N \rfloor dx \quad (2.19)$$

$[c3]^{(e)}$ = viscous drag damping matrix for the element

$$= \int_0^h X \{N\} \lfloor N \rfloor \, dx \quad (2.20)$$

$[k]^{(e)}$ = total stiffness matrix for the element

$$= [k1]^{(e)} - [k2]^{(e)} - [k3]^{(e)} \qquad (2.21)$$

$[k1]^{(e)}$ = elastic stiffness matrix for the element

$$= \int_0^h EI\{N''\}\lfloor N''\rfloor \, dx \qquad (2.22)$$

$[k2]^{(e)}$ = stiffness matrix for the element due to curvature term $\frac{\partial^2 y}{\partial x^2}$

$$= \int_0^h (Z + W x_p)\{N'\}\lfloor N'\rfloor \, dx \qquad (2.23)$$

and

$[k3]^{(e)}$ = stiffness matrix for the element due to variable curvature term $x \frac{\partial^2 y}{\partial x^2}$

$$= \int_0^h W x\{N'\}\lfloor N'\rfloor \, dx \qquad (2.24)$$

To calculate these matrices one has to choose $y^{(e)}$. The following conditions must be fulfilled while selecting this $y^{(e)}$ to ensure monotonic convergence, Huebner [9] :

(i) Completeness, i.e., all uniform states of y and its partial derivatives upto the highest order appearing in Eqn. (2.14) should have a representation in $y^{(e)}$ when in the limit, the size of the element shrinks to zero.

(ii) Compatibility, i.e., at the interfaces of the elements y and any of its partial derivatives one order less than the highest order appearing in Eqn. (2.14) must be continuous.

The following shape function, usually used for beam problems, in terms of generalized co-ordinates has been chosen for the present problem, since it satisfies the above requirements of completeness and compatibility, respectively,

$$\lfloor N \rfloor = \lfloor \xi_1^2 (3 - 2\xi_1) \quad \xi_1^2 \xi_2 h \quad \xi_2^2 (3 - 2\xi_2) \quad -\xi_1 \xi_2^2 h \rfloor , \qquad \ldots\ (2.25)$$

where $\xi_1 = 1 - \frac{x}{h}$ and $\xi_2 = \frac{x}{h}$.

Introducing the shape function into the Eqns. (2.16), (2.18), (2.19), (2.20), (2.22), (2.23) and (2.24) and integrating, one obtains

$$[m]^{(e)} = \frac{(m_r + C_m m_r)h}{420} \begin{bmatrix} 156 & 22h & 54 & -13h \\ & 4h^2 & 13h & -3h^2 \\ & & 156 & -22h \\ \text{Symmetric} & & & 4h^2 \end{bmatrix} \qquad (2.26)$$

$$[c1]^{(e)} = \frac{\mu I}{h^3} \begin{bmatrix} 12 & 6h & -12 & 6h \\ & 4h^2 & -6h & 2h^2 \\ & & 12 & -6h \\ \text{Symmetric} & & & 4h^2 \end{bmatrix} \qquad (2.27)$$

$$[c2]^{(e)} = \frac{2\,C_m\,m_f\,V}{60}\begin{bmatrix} 30 & 6h & 30 & -6h \\ -6h & 0 & 6h & -h^2 \\ -30 & -6h & -30 & 6h \\ 6h & h^2 & -6h & 0 \end{bmatrix} \qquad (2.28)$$

$$[c3]^{(e)} = \frac{Xh}{420}\begin{bmatrix} 156 & 22h & 54 & -13h \\ & 4h^2 & 13h & -3h^2 \\ & & 156 & -22h \\ \text{Symmetric} & & & 4h^2 \end{bmatrix} \qquad (2.29)$$

$$[k1]^{(e)} = \frac{EI}{h^3}\begin{bmatrix} 12 & 6h & -12 & 6h \\ & 4h^2 & -6h & 2h^2 \\ & & 12 & -6h \\ \text{Symmetric} & & & 4h^2 \end{bmatrix} \qquad (2.30)$$

$$[k2]^{(e)} = \frac{(Z + W x_p)}{30h}\begin{bmatrix} 36 & 3h & -36 & 3h \\ & 4h^2 & -3h & -h^2 \\ & & 36 & -3h \\ \text{Symmetric} & & & 4h^2 \end{bmatrix} \qquad (2.31)$$

and

$$[k3]^{(e)} = \frac{W}{30}\begin{bmatrix} 18 & 3h & -18 & 0 \\ & h^2 & -3h & -h^2/2 \\ & & 18 & 0 \\ \text{Symmetric} & & & 3h^2 \end{bmatrix} \qquad (2.32)$$

Therefore Eqn. (2.15) becomes,

$$[m]^{(e)}\{\ddot{y}\}^{ne} + [c]^{(e)}\{\dot{y}\}^{ne} + [k]^{(e)}\{y\}^{ne} + \begin{Bmatrix} -\mu I \dfrac{\partial^4 y^{(e)}}{\partial x^3\, \partial t}\Big|_p \\ 0 \\ +\mu I \dfrac{\partial^4 y^{(e)}}{\partial x^3\, \partial t}\Big|_q \\ 0 \end{Bmatrix} - \begin{Bmatrix} 0 \\ -\mu I \dfrac{\partial^3 y^{(e)}}{\partial x^2\, \partial t}\Big|_p \\ 0 \\ +\mu I \dfrac{\partial^3 y^{(e)}}{\partial x^2\, \partial t}\Big|_q \end{Bmatrix} + \begin{Bmatrix} -2 C_m m_f V \dfrac{\partial y^{(e)}}{\partial t}\Big|_p \\ 0 \\ +2 C_m m_f V \dfrac{\partial y^{(e)}}{\partial t}\Big|_q \\ 0 \end{Bmatrix} + \begin{Bmatrix} -EI \dfrac{\partial^3 y^{(e)}}{\partial x^3}\Big|_p \\ 0 \\ +EI \dfrac{\partial^3 y^{(e)}}{\partial x^3}\Big|_q \\ 0 \end{Bmatrix}$$

$$- \begin{Bmatrix} 0 \\ -EI \dfrac{\partial^2 y^{(e)}}{\partial x^2}\Big|_p \\ 0 \\ +EI \dfrac{\partial^2 y^{(e)}}{\partial x^2}\Big|_q \end{Bmatrix} + \begin{Bmatrix} -Z \dfrac{\partial y^{(e)}}{\partial x}\Big|_p \\ 0 \\ +Z \dfrac{\partial y^{(e)}}{\partial x}\Big|_q \\ 0 \end{Bmatrix} + \begin{Bmatrix} -W(x_p+x) \dfrac{\partial y^{(e)}}{\partial x}\Big|_p \\ 0 \\ +W(x_p+x) \dfrac{\partial y^{(e)}}{\partial x}\Big|_q \\ 0 \end{Bmatrix} = \{0\} \quad \ldots\ldots \quad (2.33)$$

For the whole domain of the problem, Eqn. (2.33) becomes

$$
[M]_{BB}\{\ddot{y}\}^{n} + [C]_{BB}\{\dot{y}\}^{n} + [K]_{BB}\{y\}^{n} +
\begin{Bmatrix}
-2C_m m_f V \left.\frac{\partial y^{(e)}}{\partial t}\right|_1 \\
0 \\
0 \\
\vdots \\
0 \\
2C_m m_f V \left.\frac{\partial y^{(e)}}{\partial t}\right|_{m+1} \\
0
\end{Bmatrix}
+
\begin{Bmatrix}
-Z \left.\frac{\partial y^{(e)}}{\partial x}\right|_1 \\
0 \\
0 \\
\vdots \\
0 \\
+Z \left.\frac{\partial y^{(e)}}{x}\right|_{m+1} \\
0
\end{Bmatrix}
+
\begin{Bmatrix}
0 \\
0 \\
0 \\
\vdots \\
0 \\
W m h \left.\frac{\partial y^{(e)}}{x}\right|_{m+1} \\
0
\end{Bmatrix} =
$$

$$
-\begin{Bmatrix}
-\left(EI\frac{\partial^3 y^{(e)}}{\partial x^3} + \mu I \frac{\partial^4 y^{(e)}}{\partial x^3 \partial t}\right)\Big|_1 \\
0 \\
0 \\
\vdots \\
0 \\
\left(EI\frac{\partial^3 y^{(e)}}{\partial x^3} + \mu I \frac{\partial^4 y^{(e)}}{\partial x^3 \partial t}\right)\Big|_{m+1} \\
0
\end{Bmatrix}
+
\begin{Bmatrix}
0 \\
\left(-EI\frac{\partial^2 y^{(e)}}{\partial x^2} + \mu I \frac{\partial^3 y^{(e)}}{\partial x^2 \partial t}\right)\Big|_1 \\
0 \\
\vdots \\
0 \\
\left(EI\frac{\partial^2 y^{(e)}}{\partial x^2} + \mu I \frac{\partial^3 y^{(e)}}{\partial x^2 \partial t}\right)\Big|_{m+1}
\end{Bmatrix}
\tag{2.34}
$$

where

$[M]_{BB}$ = assembled mass matrix for the whole domain before applying the boundary conditions

$[C]_{BB}$ = assembled damping matrix for the whole domain before applying the boundary conditions

and

$[K]_{BB}$ = assembled stiffness matrix for the whole domain before applying the boundary conditions.

For computational ease, Eqn. (2.34) can be rearranged as follows:

$$[M]_{BB}\{\ddot{y}\}^n + [C]_{BB}\{\dot{y}\}^n + \begin{Bmatrix} -2\,C_m\,m_f\,V\dot{y}\big|_1 \\ 0 \\ 0 \\ \vdots \\ 0 \\ +2\,C_m\,m_f\,V\dot{y}\big|_{m+1} \\ 0 \end{Bmatrix} + [K]_{BB}\{y\}^n$$

$$+ \begin{Bmatrix} -Z\,\theta\big|_1 \\ 0 \\ 0 \\ \vdots \\ 0 \\ +Z\,\theta\big|_{m+1} \\ 0 \end{Bmatrix} + \begin{Bmatrix} 0 \\ 0 \\ 0 \\ \vdots \\ 0 \\ +W\,m\,h\,\theta\big|_{m+1} \\ 0 \end{Bmatrix} =$$

$$= - \left\{ \begin{array}{c} -\left(EI \dfrac{\partial^3 y^{(e)}}{\partial x^3} + \mu I \dfrac{\partial^4 y^{(e)}}{\partial x^3\, t}\right)\Big|_1 \\ 0 \\ 0 \\ \vdots \\ 0 \\ \left(EI \dfrac{\partial^3 y^{(e)}}{\partial x^3} + \mu I \dfrac{\partial^4 y^{(e)}}{\partial x^3\, \partial t}\right)\Big|_{m+1} \\ 0 \end{array} \right\} + \left\{ \begin{array}{c} 0 \\ -\left(EI \dfrac{\partial^2 y^{(e)}}{\partial x^2} + \mu I \dfrac{\partial^3 y^{(e)}}{\partial x^2\, \partial t}\right)\Big|_1 \\ 0 \\ 0 \\ \vdots \\ 0 \\ \left(EI \dfrac{\partial^2 y^{(e)}}{\partial x^2} + \mu I \dfrac{\partial^3 y^{(e)}}{\partial x^2\, t}\right)\Big|_{m+1} \end{array} \right\} \quad \ldots\ldots \quad (2.35)$$

In Eqn. (2.35), the values $- 2 C_m m_f V$ and $+ 2 C_m m_f V$ are added up with the elements $C_{1,1}$ and $C_{2m+1,2m+1}$ of the assembled damping matrix, respectively. It should also be noted that the coefficients of θ_1 and θ_{m+1} are summed-up with the elements $K_{1,2}$ and $K_{2m+1,2m+2}$ of the assembled stiffness matrix, respectively.

After substituting the boundary conditions, Eqn. (2.35) can be written as

$$[M]\{\ddot{y}\}^n + [C]\{\dot{y}\}^n + [K]\{y\}^n = \{0\}, \qquad (2.36)$$

where $[M]$, $[C]$ and $[K]$ are the assembled mass, damping and stiffness matrices, respectively, for the whole domain of the problem, after applying the boundary conditions.

Equation of motion (2.1) derived by Paidoussis [17] is much more general than that derived earlier, Paidoussis [14], as it

takes into consideration the gravity and pressurization effects. In addition, it eliminated the error of non-inclusion of the frictional term $F_L \left(\partial y / \partial x \right)$ in the earlier work. Earlier formulation [14] is referred as "Old Formulation" and the later formulation [17] used in this chapter as "New Formulation" in the present work and are given in Appendices A and B.

The author found it fascinating to solve the old formulation problem also by the finite element method and is given in Appendix B.

2.2 COMPUTATIONAL APPROACH :

The solution of these homogeneous set of differential equations is obtained as described in Meirovitch [11] . As per this reference the inertia, stiffness and damping matrices should necessarily be symmetric to arrive at the solution. But it is not essential for the matrices [M] , [K] and [C] to be symmetric, refer Frazer, Duncan and Collar [6] .

Equation of motion of forced vibration of a damped system is

$$[M] \{ \ddot{y} (t) \} + [C] \{ \dot{y} (t) \} + [K] \{ y(t) \} = \{ Q(t) \} , \quad \ldots \quad (2.37)$$

Equations (2.37) represent a set of coupled ordinary linear differential equations which is difficult to decouple unless matrix [C] is a linear combination of matrices [M] and [K] , which can

occur in particular cases only. For a general case, equations (2.37) can be reduced to a system of first order differential equations as follows, Meirovitch [11] ,

Premultiplying Eqn. (2.37) by $[M]^{-1}$

$$\{\ddot{y}(t)\} + [M]^{-1}[C]\{\dot{y}(t)\} + [M]^{-1}[K]\{y(t)\} = [M]^{-1}\{Q(t)\} \tag{2.38}$$

Let $\{q(t)\} = \begin{Bmatrix} \{\dot{y}(t)\} \\ \{y(t)\} \end{Bmatrix}_{[2n \times 1]}$ and $\{Y(t)\} = \begin{Bmatrix} \{0\} \\ \{Q(t)\} \end{Bmatrix}_{[2n \times 1]}$, ... (2.39)

This leads to a set of 2n first order ordinary differential equations

$$[\bar{M}]\{\dot{q}(t)\} + [\bar{K}]\{q(t)\} = \{Y(t)\} , \tag{2.40}$$

where

$$[\bar{M}] = \begin{bmatrix} [0] & [M] \\ [M] & [C] \end{bmatrix} \text{ and } [\bar{K}] = \begin{bmatrix} -[M] & [0] \\ [0] & [K] \end{bmatrix} \tag{2.41}$$

are real matrices of order 2n.

From Eqn. (2.40) we obtain the homogeneous set of differential equations in matrix form as

$$[\bar{M}]\{\dot{q}(t)\} + [\bar{K}]\{q(t)\} = \{0\} \tag{2.42}$$

The solution of Eqn. (2.42) is obtained by letting

$$\{q(t)\} = e^{\lambda t}\{\emptyset\} , \tag{2.43}$$

where $\{\emptyset\}$ represents a vector consisting of 2n constant elements. Eqn. (2.43), when introduced in Eqn. (2.42), leads to the eigenvalue problem

$$[\bar{M}]\{\phi\} + [\bar{K}]\{\phi\} = \{0\} \quad , \tag{2.44}$$

which can be rewritten in the form

$$[D]\{\phi\} = \frac{1}{\lambda}\{\phi\} \quad , \tag{2.45}$$

where

$$\begin{aligned} D &= -[\bar{K}]^{-1}[\bar{M}] \\ &= \begin{bmatrix} [M]^{-1} & [0] \\ [0] & -[K]^{-1} \end{bmatrix} \begin{bmatrix} [0] & [M] \\ [M] & [C] \end{bmatrix} \\ &= \begin{bmatrix} [0] & [I] \\ -[K]^{-1}[M] & -[K]^{-1}[C] \end{bmatrix}_{[2n \times 2n]} \end{aligned} \tag{2.46}$$

plays the role of dynamical matrix. The multiplication of partitioned matrices is handled as if the submatrices were ordinary elements. The identity matrix $[I]$ in Eqn. (2.46) is of order n.

The eigenvalues of the above dynamical matrix (2.46) will in general be complex. Real parts determine the stability of the system and the imaginary parts give the frequency of vibration. If the real part is negative, the system will be stable and vice-versa. The system will have oscillatory instability (flutter) if real part is positive and imaginary part is non-zero; whereas if the imaginary part is zero, the system will undergo buckling instability.

The formulation presented in this chapter is general and proves to be versatile because the effect of various boundary

conditions (geometrical and natural) can be studied easily. Also, the effect of various system parameters such as velocity, axial tension, fluid pressure, gravity etc. on the dynamics of rods can be studied with special interest.

A computer programme has been prepared to compute the eigenvalues using built-in subroutine ZINDIA. Listing of computer programme is given in Appendix E. Computer programme has been discussed in Appendix D.

CHAPTER III

RESULTS AND DISCUSSION

The results obtained in the form of dimensionless parameters are included and discussed in this chapter. Various boundary conditions of the rod and the effect of various system parameters on the stability of the rod are illustrated in detail. Complex frequencies of the lowest four modes have been obtained as a function of the dimensionless flow velocity and Argand diagrams have been plotted. All the results are given in terms of the dimensionless parameters. Lastly, the mechanism of instability has been discussed in brief.

3.1 DIMENSIONLESS PARAMETERS

Following dimensionless parameters have been used in this work,

β = Dimensionless mass = $m_f/(m_f + m_r)$

u = Dimensionless flow velocity = $(m_f/EI)^{1/2} VL$

Γ = Dimensionless axial tension = $\bar{T} L^2/EI$

α = Dimensionless internal damping coefficient

= $\{I/ [E (m_f + m_r)]\}^{1/2} \mu / L^2$

γ = Dimensionless gravity parameter = $(m_r - m_f) g L^3/EI$

η = Dimensionless pressure parameter = $(\overline{pA}) L^2/EI$

$Re(\omega)$ = Real part of the dimensionless frequency $= \{ (m_f + m_r)/EI \}^{1/2} \omega_R L^2$

$Im(\omega)$ = Imaginary part of the dimensionless frequency

$= \{ (m_f + m_r)/EI \}^{1/2} \omega_I L^2$

α_d = Dimensionless displacement spring factor = $K_d L^3/EI$

α_t = Dimensionless rotational spring factor = $K_t L^2/EI$

c_d = Dimensionless viscous drag coefficient = $C_D L(m_f/EI)^{1/2}$

c_f = Friction drag coefficient = $(4/\pi)\, C_f$

c_b = Base drag coefficient = $(4/\pi)\, C_b$

3.2 CONVERGENCE OF THE EIGENVALUES:

Finite element analysis says that as the number of complete and compatible finite elements is increased, the results converge monotonically to the exact values. However, one has to choose finite number of finite elements. For the present work, first for every boundary condition results were obtained for a few non-dimensional velocities for various numbers of the finite elements. It was observed that for five elements results were quite acceptable for all the cases. Sample results for pinned-pinned rod and cantilever rod are shown in Table 1 and 2, for NEL from 2 to 7 and from 2 to 5, respectively, (pp.30,31). It should be noted that the change in the frequencies after NEL = 4 is negligible. Therefore, it was decided to use five finite elements for determining the results. Moreover, this saved computational time also.

TABLE 1

NUMBER OF ELEMENTS VS FREQUENCIES

PINNED-PINNED ROD ($\beta = 0.1$, $\varepsilon c_f = 1$)

(OLD FORMULATION)

Number of Elements	u = 0.0				u = 2.0				u = 6.0			
	Ist mode		2nd mode		Ist mode		2nd mode		Ist mode		2nd mode	
	Re(ω)	Im(ω)	Re(ω)	Im(ω)	Re(ω)	Im(ω)	Re(ω)	Im(ω)	Re(ω)	Im(ω)	Re(ω)	Im(ω)
2	0	9.908	0	43.817	-0.167	7.630	-0.153	42.013	-16.186 +14.093	0	0.085	22.975
3	0	9.877	0	39.945	-0.169	7.586	-0.153	37.971	-16.032 +13.186	0	0.233	14.448
4	0	9.872	0	39.634	-0.170	7.578	-0.154	37.636	-16.001 +13.016	0	0.254	13.433
5	0	9.870	0	39.543	-0.170	7.576	-0.154	37.538	-15.992 +12.966	0	0.262	13.130
6	0	9.870	0	39.510	-0.170	7.575	-0.154	37.502	-15.988 +12.947	0	0.264	13.015
7	0	9.869	0	39.495	-0.170	7.574	-0.154	37.486	-15.987 +12.939	0	0.265	12.964

TABLE 2

NUMBER OF ELEMENTS VS FREQUENCIES

CANTILEVERED ROD WITH TAPERED END ($\beta = 0.5$, $\epsilon c_f = 1$)

(NEW FORMULATION)

Number of Elements	u = 0.0				u = 2.0				u = 6.0			
	1st mode		2nd mode		1st mode		2nd mode		1st mode		2nd mode	
	Re(ω)	Im(ω)	Re(ω)	Im(ω)	Re(ω)	Im(ω)	Re(ω)	Im(ω)	Re(ω)	Im(ω)	Re(ω)	Im(ω)
2	0	3.455	0	21.836	-0.310 -1.556	0	-0.855	20.601	-10.128	4.919	3.749	9.990
3	0	3.454	0	21.725	-0.302 -1.561	0	-0.847	20.403	-10.495	4.889	4.239	9.743
4	0	3.454	0	21.689	-0.300 -1.561	0	0.843	20.346	-10.518	4.860	4.268	9.693
5	0	3.454	0	21.669	-0.300 -1.561	0	0.841	20.328	-10.524	4.851	4.275	9.677

3.3 COMPLEX FREQUENCIES OF RODS:

The dimensionless complex frequencies obtained for the present problem are plotted in Argand diagrams for different boundary conditions of the rod. The imaginary part of the dimensionless value $Im(\omega)$, which represents the frequency of vibration is plotted on the abscissa and the real part $Re(\omega)$, on the ordinate. The various parameters involved in the problem are $\alpha, \beta, \gamma, F, \delta, \eta, u, \alpha_d, \alpha_t$, c_f, c_b and c_d.

3.3.1 PINNED-PINNED ROD:

The boundary conditions for pinned-pinned rod are

$$y = 0 \quad \text{at} \quad x = 0 \quad \text{and} \quad x = L, \tag{3.1}$$

$$EI \frac{\partial^2 y}{\partial x^2} + \mu I \frac{\partial^3 y}{\partial x^2 \partial t} = 0 \quad \text{at} \quad x = 0, \tag{3.2}$$

$$EI \frac{\partial^2 y}{\partial x^2} + \mu I \frac{\partial^3 y}{\partial x^2 \partial t} = 0 \text{ at } x = L. \tag{3.3}$$

Since pinned-pinned rods are of considerable practical interest as compared to the cantilevered rods and clamped-clamped rods; this boundary condition is studied in detail and the effect of various dimensionless parameters on the stability of the rod is discussed.

3.3.1.1 OLD FORMULATION:

In this old formulation, transverse component of tangential frictional force F_L is neglected, see Paidoussis [14] and Appendix B. Fig. 3.1 shows the dimensionless complex frequencies of the lowest three modes of a system as a function of the dimensionless

flow velocity u , for $\beta = 0.1, \varepsilon c_f = 1, \Gamma = 0, = C_m = 1$. These results were compared with the results of Paidoussis [14] and it was observed that results were matching with those of available results except for certain velocity ranges, i.e., in the first mode for $u \geq 3$ and and in second mode for $5 < u < 6$. Careful study of the available results indicated that there was ill-conditioning for the above mentioned velocity ranges, i.e., for small changes in u, a large change in complex frequencies was observed. This led the author to believe that there is ill-conditioning in the system in these velocity ranges and the convergence is incomplete for five elements. Therefore, the results for these velocity ranges, where ill-conditioning was believed to be present, were studied by increasing the number of elements from 2 to 8. These results are tabulated in Table 3.

Still for 8 elements there is some difference in the present and Paidoussis's[14] results in these velocity ranges. Moreover, the results of Paidoussis [14] may also not be reliable for the ill-conditioned ranges.

3.3.1.2 NEW FORMULATION:

Case (A) : $\beta = 0.1, \varepsilon c_f = 1, \delta = C_m = 1, c_d = \alpha = \gamma = \eta = \Gamma = 0$.

Fig. 3.2 shows the dimensionless complex frequencies of the lowest three modes of the system as a function of the dimensionless flow velocity u. The results match very well with those obtained by Paidoussis [17] except for certain ranges of u, where ill-conditioning was observed to be present, i.e., $6 \leq u \leq 6.5$ in the second mode

TABLE 3

NUMBER OF ELEMENTS VS FREQUENCIES

PINNED-PINNED ROD ($\beta = 0.1, \varepsilon c_f = 1$)

(OLD FORMULATION)

Number of Elements	u = 3.136 Ist mode		u = 3.137 Ist mode		u = 3.1138 Ist mode		u = 3.14 Ist mode		u = 3.145 Ist mode		u = 5.5 2nd mode	
	Re(ω)	Im(ω)	Re(ω)	Im(ω)	Re(ω)	Im(ω)	Re(ω)	Im(ω)	Re(ω)	Im(ω)	Re(ω)	Im(ω)
2	0.289	0.886	0.289	0.851	0.290	0.814	0.290	0.735	0.290	0.485	0.043	21.905
3	0.298	0.392	0.298	0.305	0.298	0.179	-0.000 +0.598	0	-0.928 +0.329	0	0.101	20.929
4	0.299	0.211	-0.172 -0.427	0	-0.022 -0.577	0	-0.746 +0.145	0	-1.011 +0.409	0	0.109	20.262
5	0.300	0.119	-0.084 -0.516	0	-0.628 +0.027	0	-0.779 +0.178	0	-1.023 +0.429	0	0.112	20.067
6	0.300	0.055	-0.059 -0.541	0	-0.645 +0.043	0 0	-0.791 +0.189	0	-1.040 +0.437	0	0.113	19.993
7	-0.256 -0.343	0	-0.050 -0.550	0	-0.652 +0.051	0	-0.796 +0.194	0	-1.043 +0.440	0	0.113	19.961
8	-0.238 -0.362	0	-0.046 -0.554	0	-0.655 -0.053	0	-0.789 +0.196	0	-1.044 +0.441	0	0.113	19.945

and $7 \leq u \leq 10$ in the third mode. Studying Fig. 3.2 and Table 3 it was thought that not much will be gained by increasing the number of finite elements.

It is observed that small flow velocities damp free motions of the rod. It is also noted that the behavior of the pinned-pinned rod is changed a lot by the corrections made in the frictional force terms. In the older formulation, Fig. 3.1, buckling occurs in the first mode only and flutter occurs in second and third modes. Whereas, in the new formulation, Fig. 3.2, buckling can occur in all the three modes and there is coupled mode flutter at $u \simeq 6.48$ (first mode for $u > 6.48$. It may be noted that there is no coupled-mode flutter for $u > 6.48$, as wrongly interpreted by Paidoussis [17] .

Case (B) : $\beta = 0.48$, $\varepsilon c_f = 0.25$, $\delta = C_m = 1$, $c_d = \alpha = \gamma = \eta = \Gamma = 0$.

Fig. 3.3 shows the dimensionless complex frequencies of the lowest three modes for the system as a function of the dimensionless flow velocity u. Considerably good agreement of the results with those obtained by Paidoussis [17] is observed. In the first mode ill-conditioning is present for $3 < u < 3.25$ and $6.25 < u < 6.4$. Slight discrepency is observed in the results for $6.25 < u < 6.4$.

Results for $\beta = 0.1$ and keeping the other parameters same are also shown in Fig. 3.3 for u upto 3.1. It is interesting to note that the increase in β tends to increase the damping in the system for small values of u. In fact, it can be seen from the coefficient of $\frac{\partial Y}{\partial x}$ from Eqn. (2.6).

In this case second mode does not cross $Im(\omega)$ - axis. Thus no buckling occurs in the second mode. The first mode branch first crosses $Im(\omega)$ - axis through the origin at $u \simeq 3.14$ and again at $u \simeq 6.29$. It leaves the real axis at $u \simeq 6.295$ and flutter occurs for $u \geq 6.295$. There is no coupled-mode flutter, as wrongly interpreted by Paidoussis [17] .

Case (C) : EFFECT OF TENSION: $\beta = 0.1$, $\varepsilon\, c_f = 0.25$, $\Gamma = 10$, $\delta = C_m = 1$, $c_d = \alpha = \gamma = \eta = 0$.

Fig. 3.4 shows the dimensionless complex frequencies of the lowest three modes for the system as a function of dimensionless flow velocity u. For this case, Paidoussis [17] obtained the values of first buckling velocity, second buckling velocity and the critical velocity for coupled-mode flutter as $u_{b1} = 4.455$, $u_{b2} = 7.04$ and $u_{c0} = 7.11$. The author obtained these values as $u_{b1} \simeq 4.456$, $u_{b2} \simeq 7.045$ and $u_{c0} \simeq 7.12$. This slight discrepency between the results is due to ill-conditioning in the system near these velocities. It is observed that externally applied axial tension has stabilizing effect, i.e., it raises the critical flow velocities.

Case (D) : EFFECT OF INTERNAL DAMPING: $\beta = 0.1$, $\varepsilon\, c_f = 0.25$, $\alpha = 0.003$, $\delta = C_m = 1$, c_d $\gamma = \eta = \Gamma = 0$.

Fig.3.5 shows the dimensionless complex frequencies for the system as a function of the dimensionless flow velocity u. The dynamic behavior is very similar to the Case (A), see Fig. 3.2.

The first and second buckling velocities, as obtained by Paidoussis [17] are $u_{b1} = 3.143$ and $u_{b2} = 6.28$ and the critical velocity for coupled-mode flutter is $u_{c0} = 6.52$. In the present case, the author obtained these velocities as $u_{b1} \simeq 3.141$, $u_{b2} \simeq 6.29$ and $u_{c0} \simeq 6.35$. Slight discrepency in these results is due to ill-conditioning near these velocities. It is noted from Fig. 3.5 that coupled-mode flutter occurs at $u \simeq 6.35$ and flutter occurs in the first mode for $u > 6.35$.

Case (E) : EFFECT OF GRAVITY: $\beta = 0.1$, $\varepsilon c_f = 0.25$, $\gamma = 10$,

$$\delta = C_m = 1, \quad c_d = \alpha = \eta = \Gamma = 0.$$

Fig. 3.6 shows the dimensionless complex frequencies for the system as the function of the dimensionless flow velocity u. The first and second buckling velocities obtained by Paidoussis [17] are $u_{b1} = 3.107$, $u_{b2} = 6.30$ and the critical velocity for coupled-mode flutter is $u_{c0} = 6.44$. The author obtained these values as $u_{b1} \simeq 3.2$, $u_{b2} \simeq 6.3$ and $u_{c0} \simeq 6.45$. Here also ill-conditioning is present for the velocity ranges $3.1 < u < 3.5$ and $6 < u < 6.5$. It is observed that the inclusion of gravity parameter slightly reduces the values of $\mathrm{Im}(\omega)$ while the effect on $\mathrm{Re}(\omega)$ is negligible.

3.3.2 CLAMPED-CLAMPED ROD:

The boundary condition for clamped-clamped rod are

$$y = 0 \quad \text{at} \quad x = 0 \quad \text{and} \quad x = L, \tag{3.4}$$

$$y' = 0 \quad \text{at} \quad x = 0 \quad \text{and} \quad x = L, \tag{3.4}$$

3.3.2.1 OLD FORMULATION:

Fig. 3.7 shows the dimensionless complex frequencies of the lowest three modes for the system as a function of the dimensionless flow velocity u, for $\beta = 0.1$, $\varepsilon\, c_f = 1$, $\delta = c_m = 1$, $\Gamma = 0$. Results obtained by Paidoussis [14] are also shown in the same figure. It is observed that the results do not match. In this case no ill-conditioning is observed in the present work or Paidoussis's work [14]. Author's results are correct as the deck used for pinned-pinned rod, modified for the clamped-clamped case was used. Correct results for $u = 0$ confirmed that the boundary conditions were applied correctly.

It is observed that buckling will occur at $u \simeq 6.25$ in the first mode which contradicts the earlier result, Paidoussis [14]. Buckling does not occur in second and third modes. Flutter instability occurs in second mode at $u \simeq 7.5$ and in third mode at $u \simeq 10.7$. It is interesting to note that third mode regions stability at $u \simeq 11.6$.

3.3.2.2 NEW FORMULATION:

Fig. 3.8 shows the dimensionless complex frequencies of the

lowest three modes for the system as a function of the dimensionless flow velocity u, for $\beta = 0.1, \varepsilon\ c_f = 1, \delta = C_m = 1, c_d = \alpha = \gamma = \eta = \Gamma = 0$. Compering this with Fig. 3.7 it is seen that due to inclusion of transverse component of frictional force, F_L, the behavior changes considerably. Now instability occurs by buckling in its first mode at $u \simeq 6.25$ and in the third mode at $u \simeq 12$. And it is interesting to note that there is no flutter instability when new formulation is used.

3.3.3 CANTILEVER ROD WITH TAPERED FREE END:

The boundary conditions for a cantilever rod with tapered free end are, see Appendix C,

$$y = y' = 0 \quad \text{at} \quad x = 0 \tag{3.6}$$

$$EI \frac{\partial^3 y}{\partial x^3} + \mu I \frac{\partial^4 y}{\partial x^3 \partial t} + f\ m_f V \left(\frac{\partial y}{\partial t} + V \frac{\partial y}{\partial x}\right) - (m_r + f\ m_f) x_e \frac{\partial^2 y}{\partial t^2} = 0 \tag{3.7}$$

and $$EI \frac{\partial^2 y}{\partial x^2} + \mu I \frac{\partial^3 y}{\partial x^2 \partial t} = 0, \text{ at } x = L, \tag{3.8}$$

where $$x_e = \frac{1}{A} \int_{L-l}^{L} A(x)\, dx.$$

3.3.3.1 OLD FORMULATION:

Fig. 3.9 shows the dimensionless complex frequencies of the lowest four modes for the system as a functions of dimensionless flow velocity u, for $\beta = 0.5$, $\varepsilon c_f = 1$, $\delta = 0$, $C_m = 1$, $f = 0.8$, $x_e/L = 0.01$,

$\Gamma = 0$. Results match completely with those obtained by classical methods, Paidoussis [14] . Both the results are shown in Fig. 3.9.

Here, it is important to note that the column matrices $\{ \left| N_i \, 2 m_f V \frac{\partial y^{(e)}}{\partial t} \right|_0^h \}$, $\{ \left| N_i \, Z \frac{\partial y^{(e)}}{\partial x} \right|_0^h \}$, $\{ \left| N_i \, W (x_p + x) \frac{y^{(e)}}{x} \right|_0^h \}$ and $\{ \left| N_i \left(EI \frac{\partial^3 y^{(e)}}{\partial x^3} + \mu I \frac{\partial^4 y^{(e)}}{\partial x^3 \, t} \right) \right|_{x=L} \}$ found in Eqn. (2.14) must be taken into consideration in mass, damping and stiffness matrices, as shown by Deb [26] . In the analysis these can not be neglected as suggested by Szabo and Lee [24] .

3.3.3.2 NEW FORMULATION:

Fig. 3.10 shows the dimensionless complex frequencies of the lowest four modes for the system as a function of dimensionless flow velocity u, for $\beta = 0.5$, $\varepsilon c_f = 1$, $\delta = 0$, $c_m = 1$, $f = 0.8$, $x_e/L = 0.01$, $c_b = \alpha = \eta = \gamma = c_d = 0$. Complete agreement was observed with the results of Paidoussis [17] upto $u = 8$. After $u > 8$, ill-conditioning was observed and for this velocity range, the convergence was studied by increasing the number of finite elements from 2 to 9. Results are tabulated in Table 4. Also in Fig. 3.10, for $u > 8$, results with NEL = 5, NEL = 8 and the results obtained by Paidoussis [17] are shown. Satisfactory convergence is not observed for $u > 8$ because of ill-conditioning.

Comparing the Figs. 3.9 and 3.10, it is observed that there is no basic change in the behavior of the system by including the

TABLE 4

NUMBER OF ELEMENTS VS FREQUENCIES

CANTILEVERED ROD WITH TAPERED END($\beta = 0.5, \varepsilon\, c_f = 1$)

(NEW FORMULATION)

Number of Elements	u = 8.25		u = 8.5				u = 8.625		u = 8.688		u = 8.81	
	3rd mode		2nd mode		3rd mode		2nd mode		2nd mode		2nd mode	
	Re(ω)	Im(ω)	Re(ω)	Im(ω)	Re(ω)	Im(ω)	Re(ω)	Im(ω)	Re(ω)	Im(ω)	Re(ω)	Im(ω)
2	-2.063	55.588	6.395	14.517	-1.758	54.068	6.115	14.894	5.948	15.092	5.569	15.493
3	-1.080	38.063	4.591	15.632	-0.375	35.716	3.740	16.328	3.189	16.718	1.763	17.562
4	-0.352	34.891	2.805	16.163	0.953	32.041	1.118	16.909	-0.047	17.181	-2.785	17.110
5	-0.115	33.930	2.190	16.264	1.433	30.984	-0.183	16.889	-1.136	16.981	-3.944	16.514
6	-0.023	33.549	1.939	16.296	1.631	30.573	-0.792	16.846	-1.552	16.856	-4.364	16.262
7	0.018	33.376	1.823	16.309	1.723	30.387	-0.363	16.820	-1.737	16.793	-4.550	16.146
8	0.039	33.289	1.765	16.315	1.770	30.293	-0.449	16.805	-1.829	16.759	-4.642	16.086
9	0.050	33.241	1.733	16.318	1.795	30.242	-	-	-	-	-4.692	16.054

transverse component of the tangential frictional force F_L in the new formulation. Buckling occurs in first mode at $u_b \simeq 2.04$ and flutter occurs at $u_{c1} \simeq 5.15$ in the second mode and at $u_{c2} \simeq 8.25$ in the third mode.

It should be noted that the results can not be relied upon for velocities $u > 8$, as ill-conditioning occurs in this velocity range.

3.4 THE MECHANISM OF INSTABILITY:

After studying the various results, the mechanism of various hydroelastic instabilities for rods subjected to external flows may be explained in brief as follows:

3.4.1 BUCKLING INSTABILITIES:

It can be seen that the term $m_f V^2 \frac{\partial^2 y}{\partial x^2}$ in $Z \frac{\partial^2 y}{\partial x^2}$ of the governing equation of motion, Eqn. (2.6), behaves more or less as an equivalent compressive force which increases with the increase in flow velocity; thus reducing natural frequencies of the system. It is possible that for certain velocity, frequencies may become zero causing buckling instability.

For pinned-pinned and clamped-clamped rods one may regard the term $Z \frac{\partial^2 y}{\partial x^2}$ as a generalized centrifugal force; when this force overcomes the flexural restoring forces, the rod buckles. For cantilevered rods with tapered free end buckling may occur when the lift

force generated at the inclined tapered free end overcomes the restoring flexural forces. Although these effects are modified by the presence of viscous forces, they remain dominant so far buckling instabilities are concerned, Paidoussis [17].

3.4.2 FLUTTER INSTABILITIES:

Oscillatory instabilities can be explained by considering the energy balance. When the energy transfer from fluid to rod and vice-versa, in the course of one cycle of oscillation, exactly balance, the condition is said to have neutral instability, i.e., dynamic equilibrium. But when the energy transfer from fluid to the rod is more than the energy transfer from rod to the fluid, the amplitude increases without limit causing flutter. In the opposite case oscillations are damped.

Paidoussis and Issid 27 have shown that conservative systems can only be subjected to coupled - mode flutter type of instability, i.e., frequencies of two modes are equal, in addition to buckling type of instability. But author finds that conservative system can also be subjected to uncoupled flutter, see Figs. 3.2, 3.3, 3.4, 3.5 and 3.6. It is left for future workers to explain this.

For detailed study of mechanism of instability one may see Refs. [14, 17, 27].

CHAPTER IV

CONCLUSIONS

In this chapter, the summary of the analysis made and the conclusions arrived at are illustrated as follows:

1. The finite element models developed for the new and old formulations are correct as the results obtained for the above mentioned formulations match quite well with those obtained earlier by classical methods for the cases of pinned-pinned rods and cantilever rods with tapered free end.

   However, for certain ranges of the flow velocities, ill-conditioning is present in the system for the pinned-pinned rods and cantilever rods with tapered free end. For these velocity ranges, the results obtained by finite element method and classical method may not be reliable.

   By increasing the number of finite elements the results do not converge for ill-conditioned velocity ranges for the cases of pinned-pinned rods and cantilever rods with tapered free end. It is observed that in general the imaginary part of the complex frequency converges while the real part shows little divergence.

2. The column matrices $\left\{ \left| N_i \, 2 m_f V \frac{\partial y^{(e)}}{\partial t} \right|_0^h \right\}$, $\left\{ \left| N_i \, Z \frac{\partial y^{(e)}}{\partial x} \right|_0^h \right\}$, $\left\{ \left| N_i \, W(x_p+x) \frac{\partial y}{\partial x} \right|_0^h \right\}$ and $\left\{ \left| N_i \left(EI \frac{\partial^3 y^{(e)}}{\partial x^3} + \mu I \frac{\partial^4 y}{\partial x^3 \partial t} \right) \right|_{x=L} \right\}$ found in Eqn. (2.14), help in introducing natural boundary conditions explicitly. These must be included in mass, damping and stiffness matrices. These column matrices can not be neglected as suggested by Szabo and Lee [24] .

3. For rods with pinned-pinned ends, coupled-mode flutter occurs for one particular velocity only, i.e., at critical velocity for coupled-mode flutter, beyond which ordinary flutter occurs. This contradicts the theory presented by Paidoussis and Issid [27] that apart from buckling, the conservative systems can only be subjected to coupled-mode flutter. It is left for the forthcoming researchers to explain.

4. The results for clamped-clamped rod for old formulation are corrected. Early results obtained by classical methods, Paidoussis [14] , show the absence of buckling in the first mode. Whereas the results obtained by finite element method indicated that buckling will occur in the first mode and the critical velocity for buckling has been found to be very close to the first buckling velocity for conservative systems obtained by using Euler's method, Paidoussis and Issid[27] .

5. Results for clamped-clamped rod for new formulation are plotted. The behavior of the clamped-clamped rod changes a lot by the inclusion of transverse component of tangential frictional force. Flutter instability does not occur in this case, only buckling instability occurs in first and third mode.

6. The finite element method with Galerkin's approach proves to be very versatile and flexible, because it gives a strong means to account explicitly for the natural boundary conditions and geometrical boundary conditions.

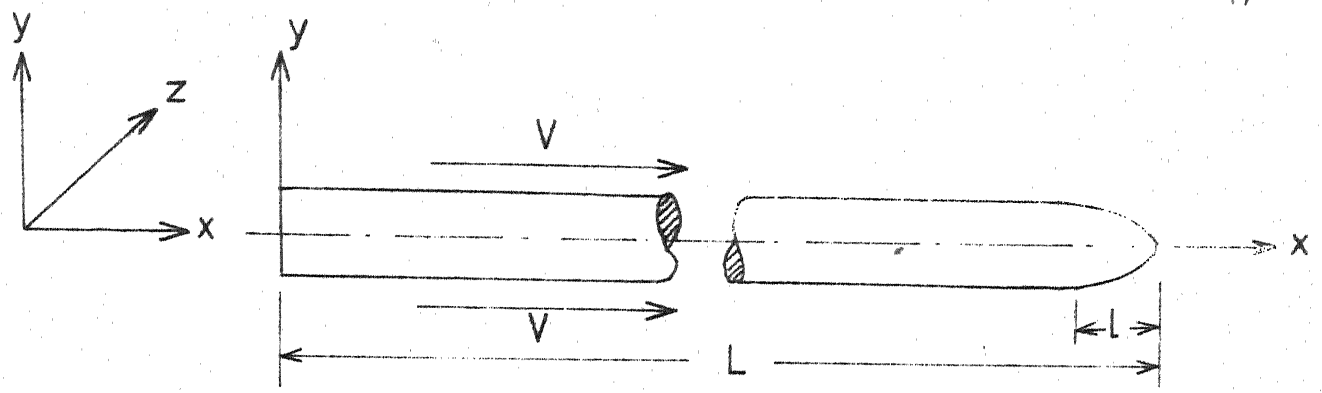

(a) Diagram of a clamped-free rod with tapered end in parallel flow

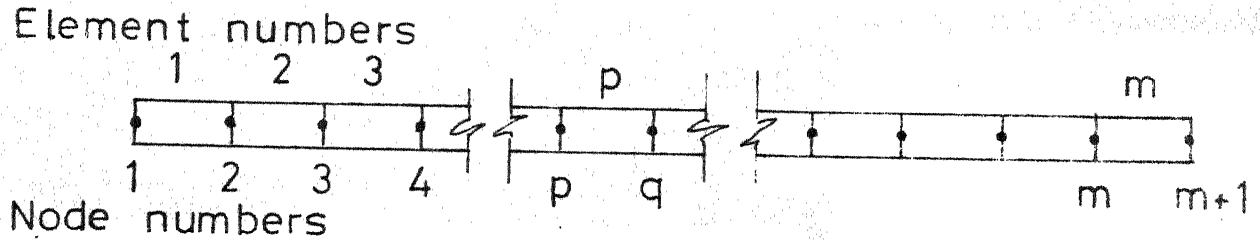

(b) Rod divided into m elements with m+1 nodes

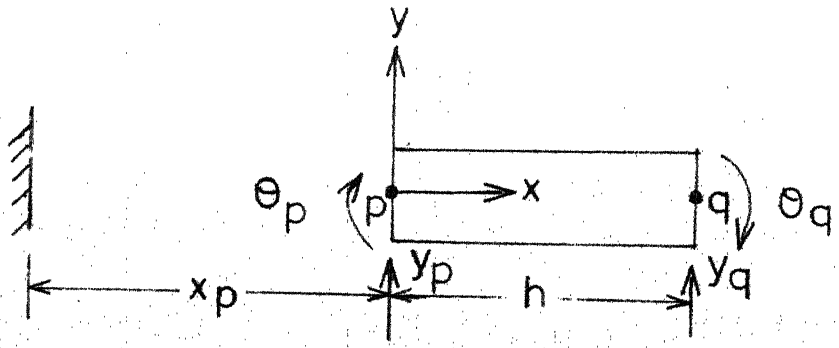

(c) Typical finite element of length h

Fig.1 Rod and its finite element representation

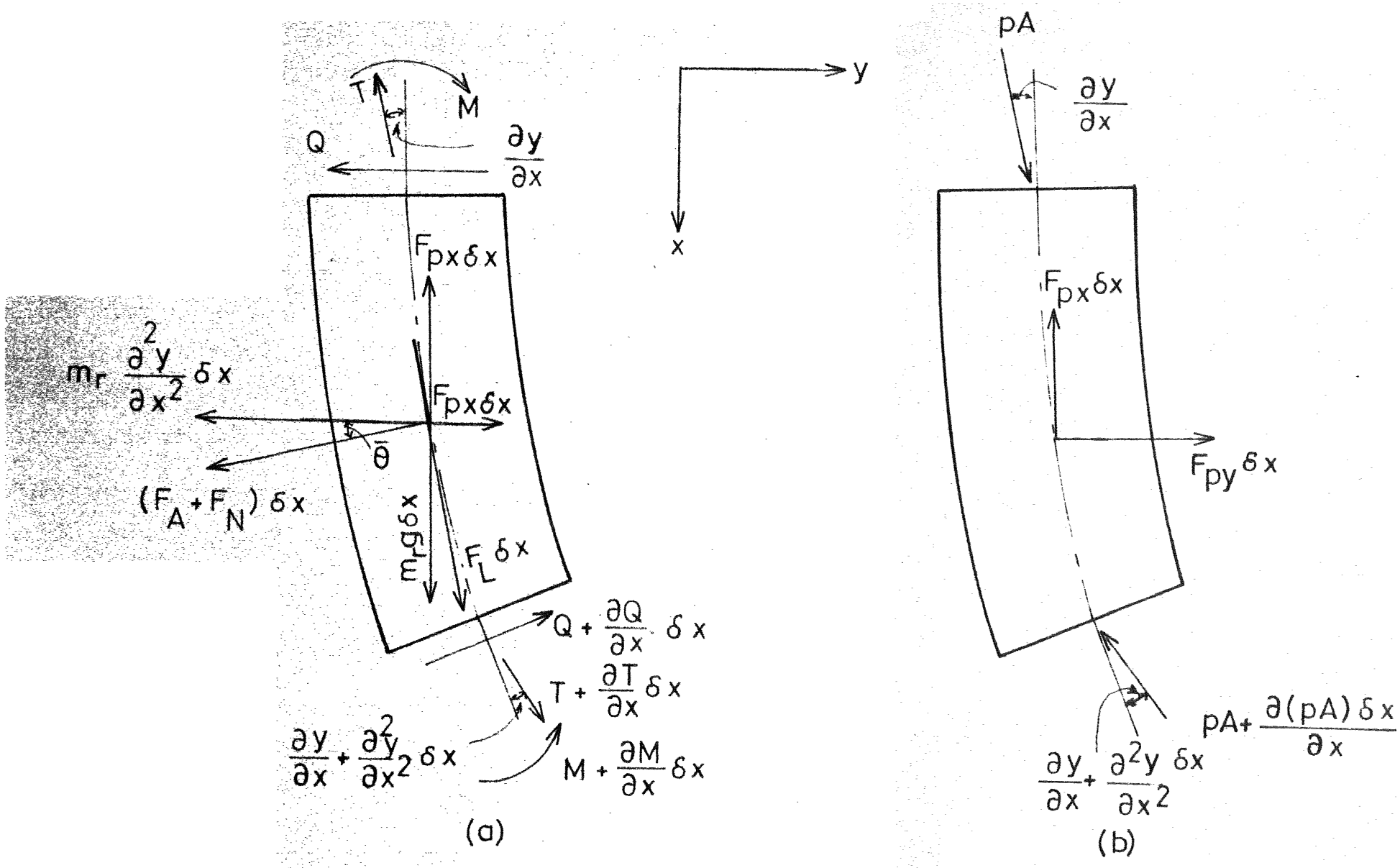

Fig. 2 (a) Forces and moments acting on an element of the rod; (b) an equivalent rigid element surrounded by fluid

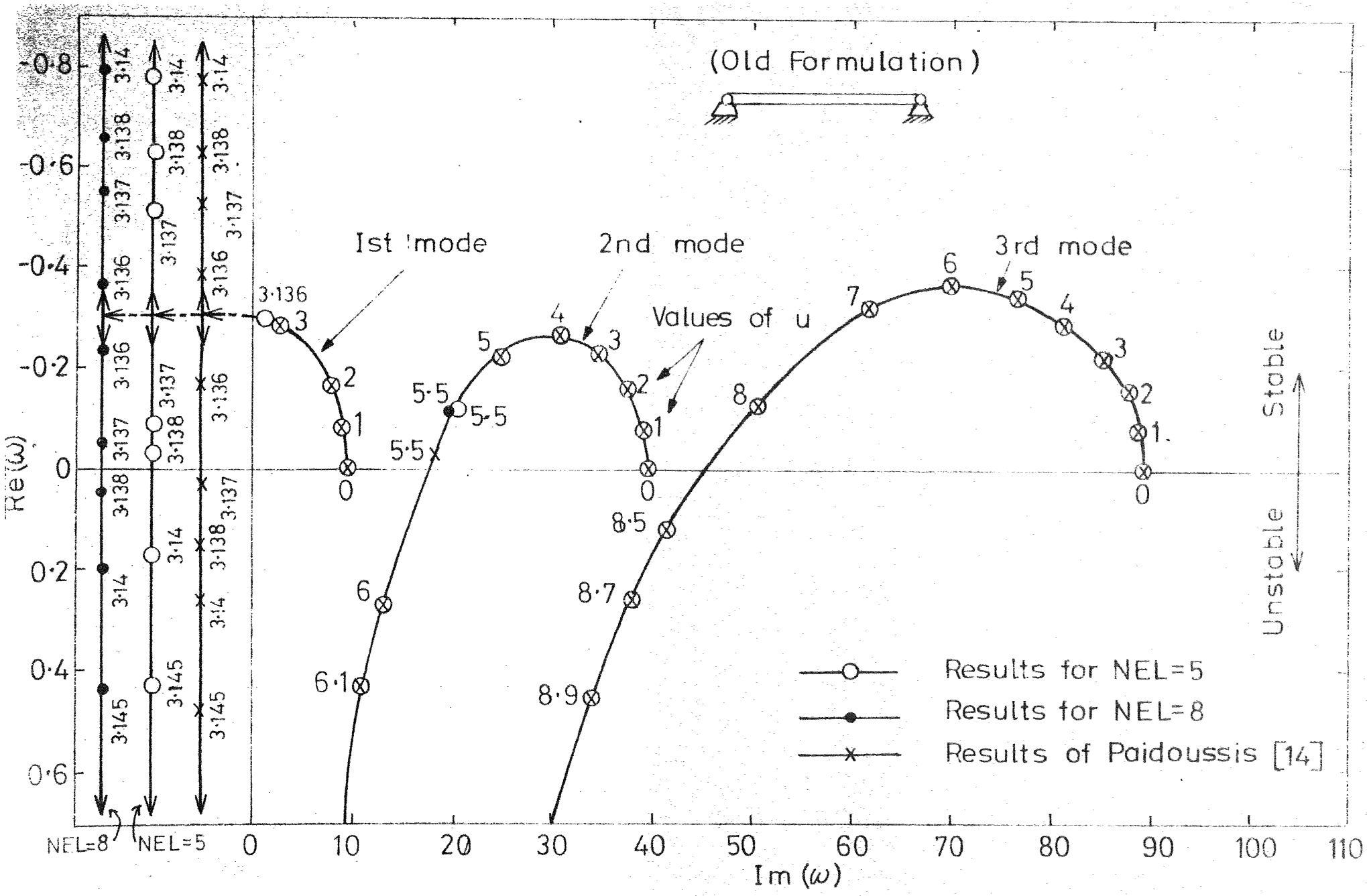

Fig. 3·1 The dimensionless complex frequency of a pinned-pinned rod as a function of the dimensionless flow velocity u, for $\beta = 0{\cdot}1$, $\varepsilon c_f = 1, \delta = Cm = 1$, $T = 0$, NEL = 5

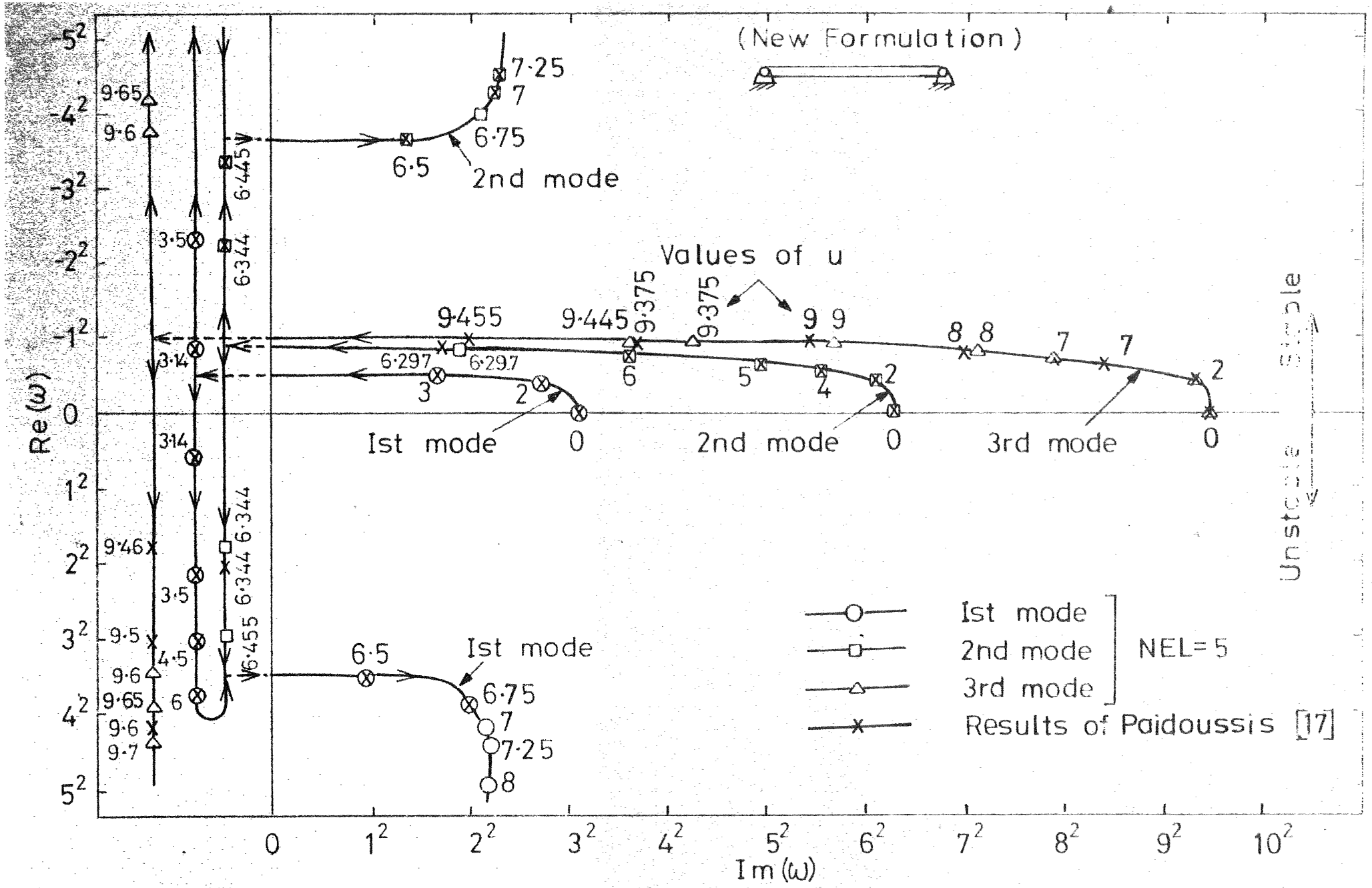

Fig. 3·2 The dimensionless complex frequency of a pinned-pinned rod as a function of the dimensionless flow velocity u, for $\beta = 0{\cdot}1$, $\varepsilon c_f = 1$, $\delta = Cm = 1$, $c_d = \alpha = \gamma = \eta = T = 0$, NEL = 5

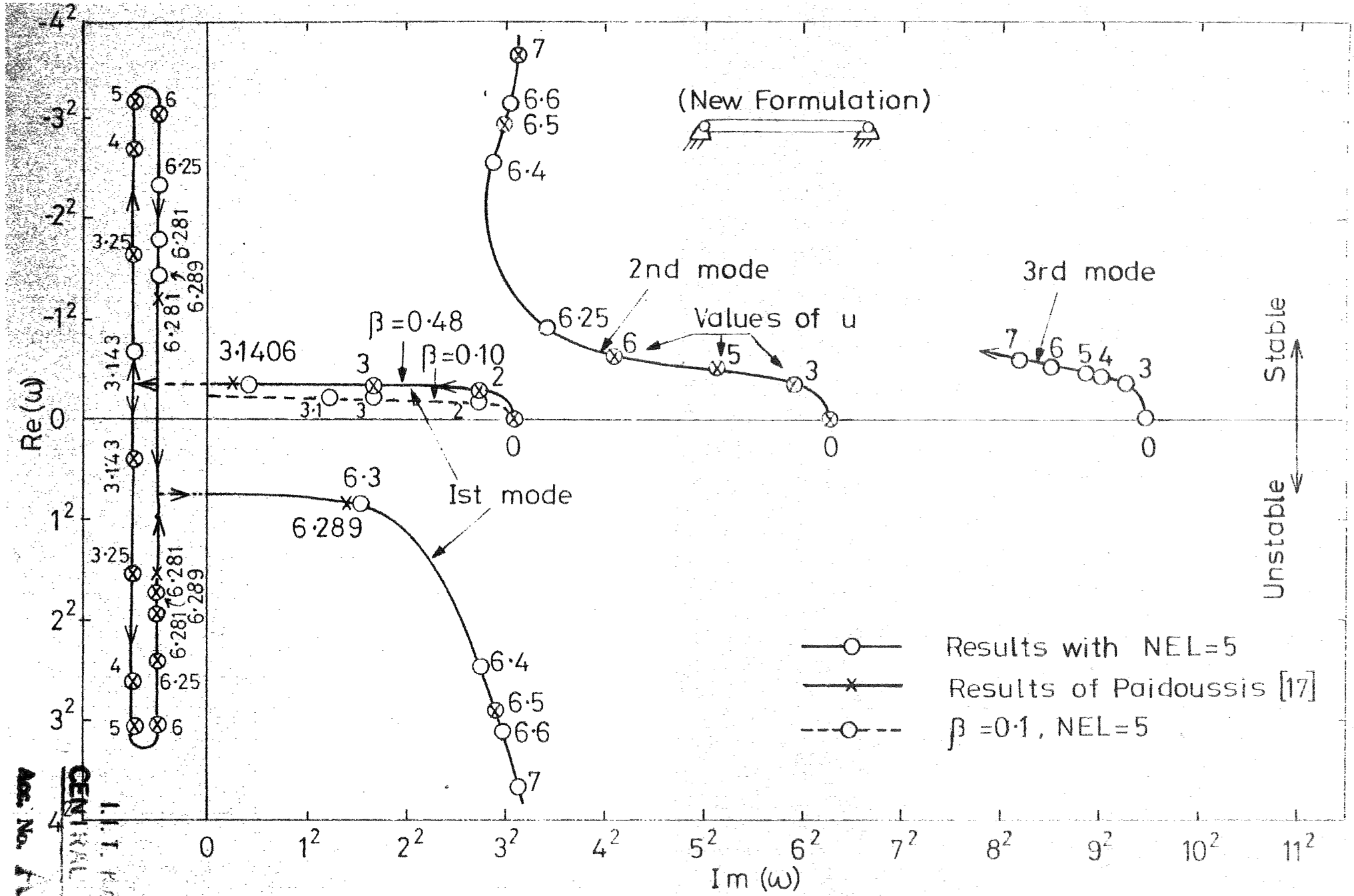

Fig. 3·3 The dimensionless complex frequency of a pinned-pinned rod as a function of the dimensionless velocity u, for $\beta = 0{\cdot}48$, $\varepsilon c_f = 0{\cdot}25$, $\delta = Cm = 1$, $c_d = \alpha = \gamma = \eta = T = 0$, NEL=5

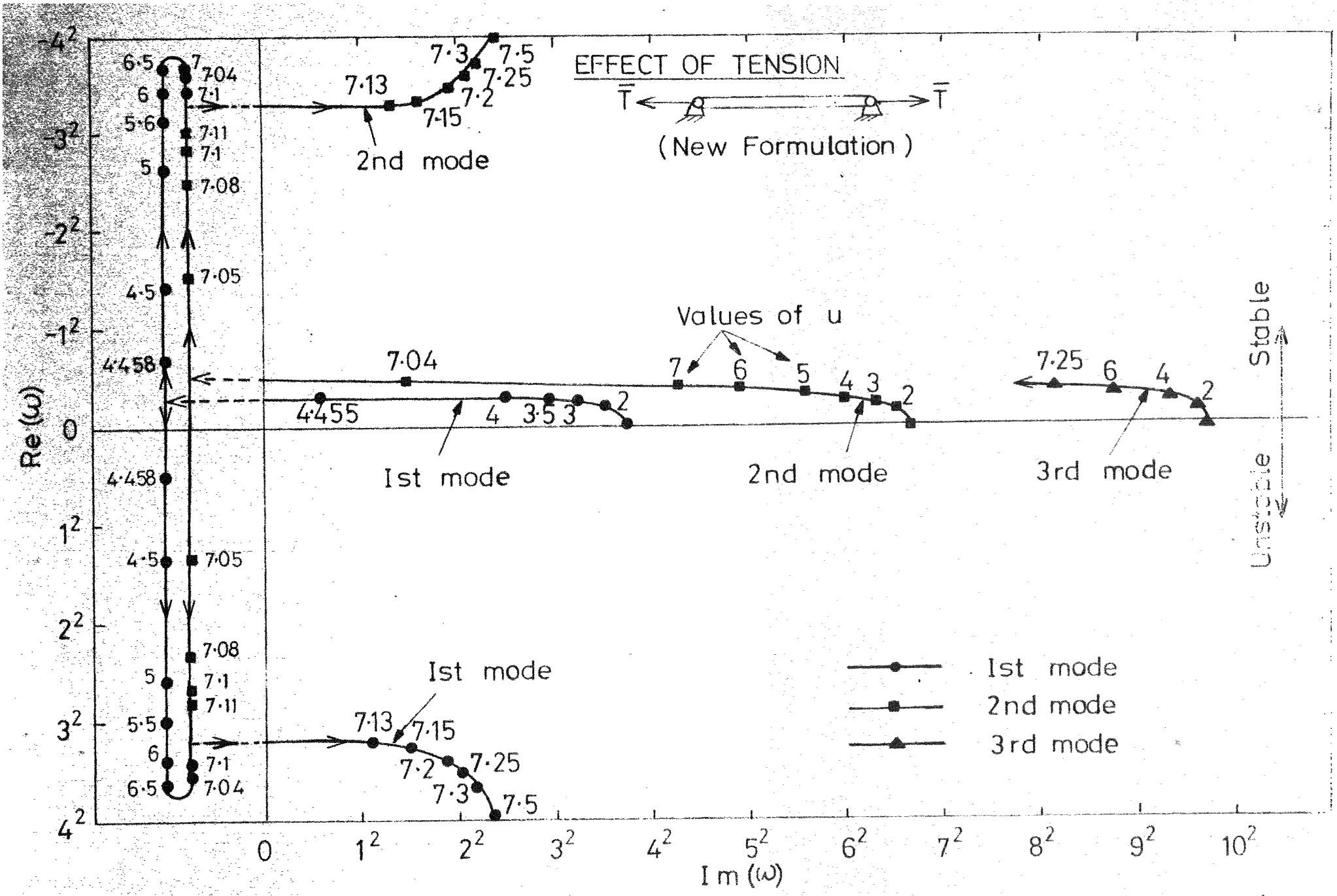

Fig. 3·4 The dimensionless complex frequency of a pinned-pinned rod as a function of the dimensionless flow velocity u, for $\beta = 0{\cdot}1$, $\varepsilon c_f = 0{\cdot}25$, $T = 10$, $\delta = C_m = 1$, $c_d = \alpha = \gamma = \eta = 0$, NEL = 5

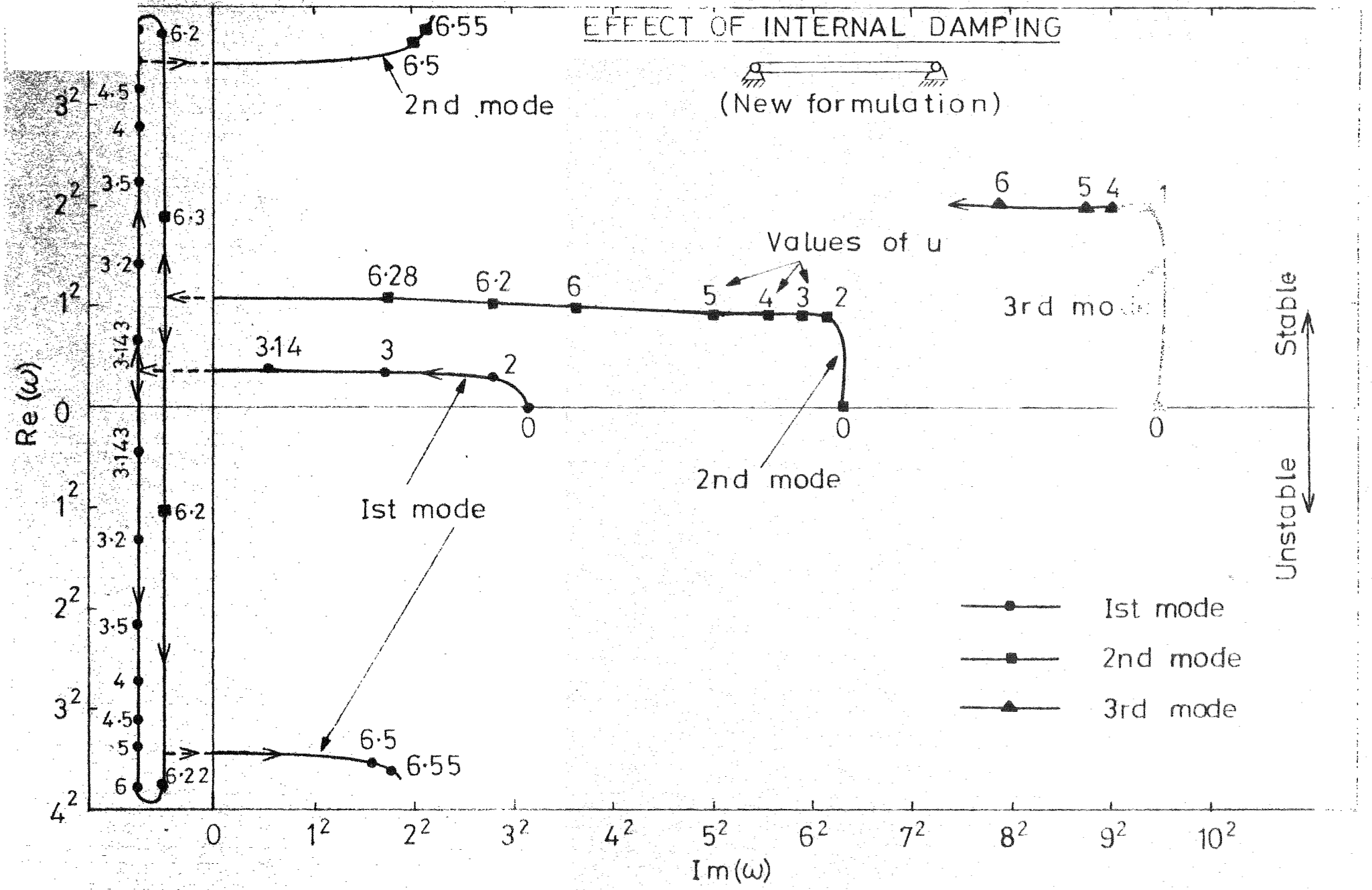

Fig. 3·5 The dimensionless complex frequency of a pinned-pinned rod as a function of the dimensionless flow velocity u, for $\beta = 0{\cdot}1$, $\varepsilon c_f = 0{\cdot}25$, $\alpha = 0{\cdot}003$, $\delta = Cm - 1$, $c_d = \gamma = \eta = \Gamma = 0$, NEL = 5

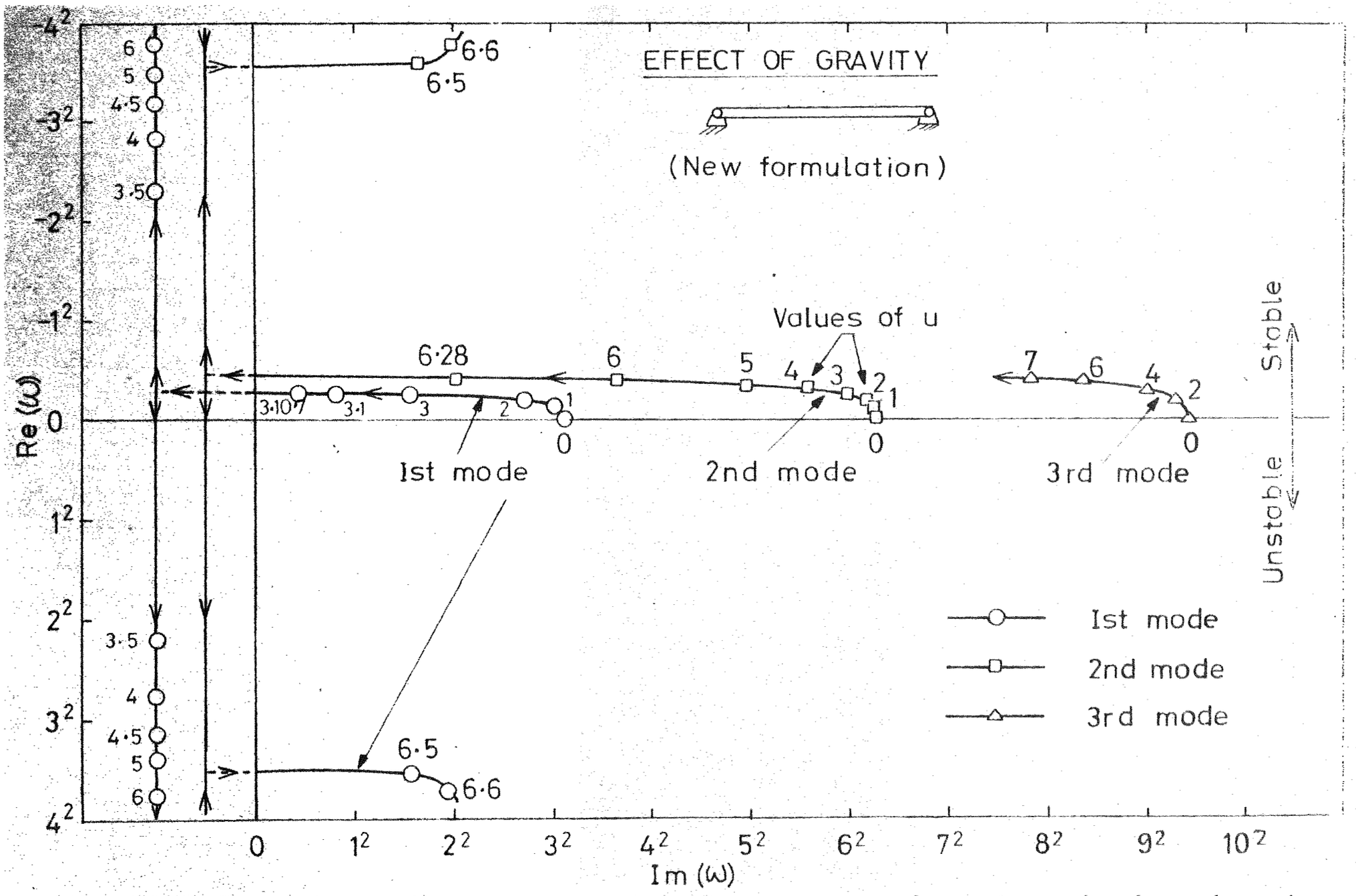

Fig. 3·6 The dimensionless complex frequency of a pinned-pinned rod as a function of the dimensionless flow velocity u, for $\beta = 0{\cdot}1$, $\varepsilon c_f = 1$, $\gamma = 10$, $\delta = C_m = 1$, $c_d = \alpha = \eta = \Gamma = 0$, NEL = 5

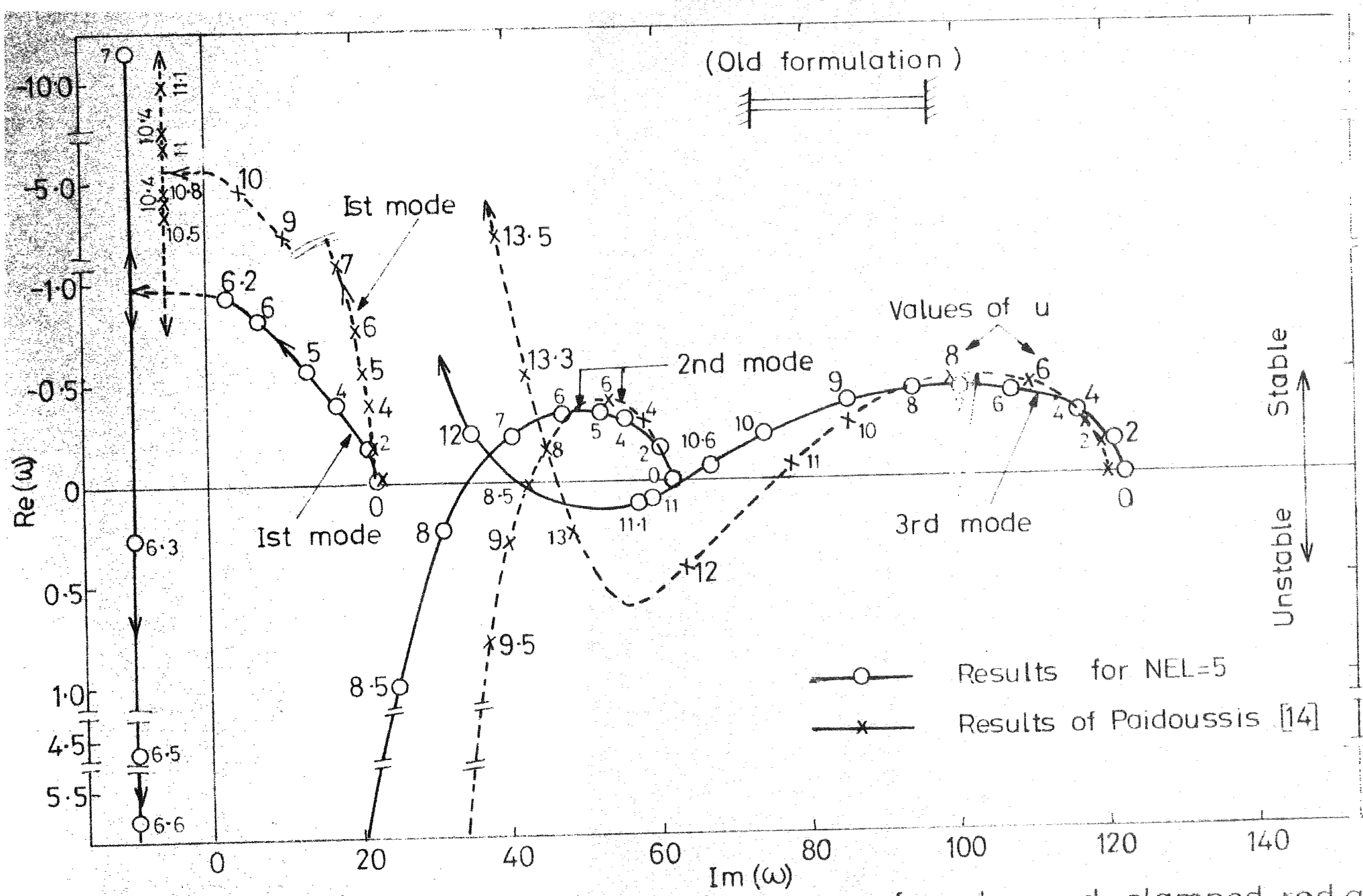

Fig. 3·7 The dimensionless complex frequency of a clamped-clamped rod as a function of the dimensionless flow velocity u, for $\beta = 0{\cdot}1$, $\varepsilon c_f = 1$, $\delta = Cm = 1$., $\Gamma = 0$, NEL=5

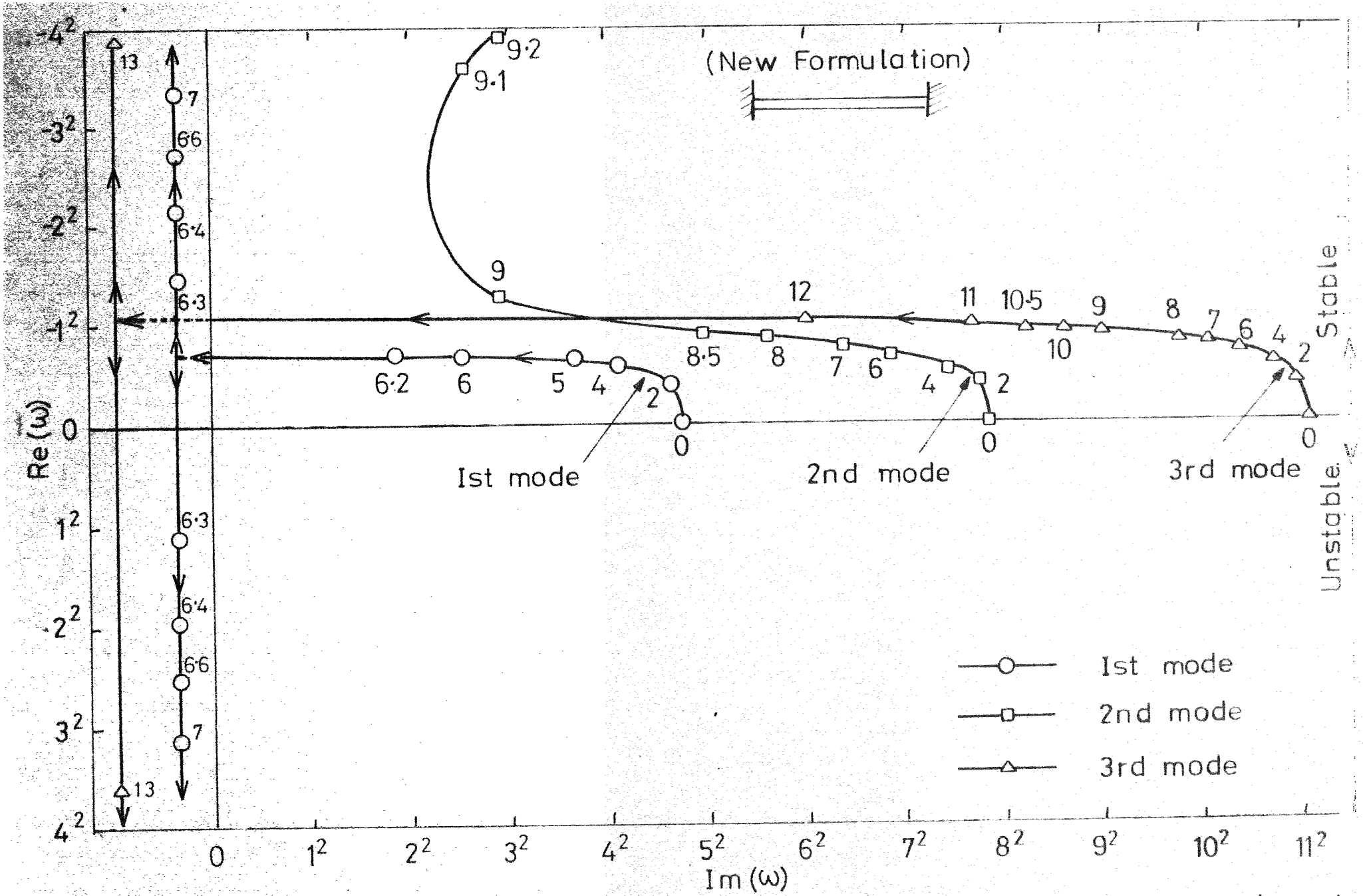

Fig. 3·8 The dimensionless complex frequency of a clamped-clamped rod as a function of the dimensionless flow velocity u, $\beta = 0{\cdot}1$, $\varepsilon c_f = 1$, $\delta = 1$, $c_d = \alpha = \gamma = n = \Gamma = 0$, NEL = 5

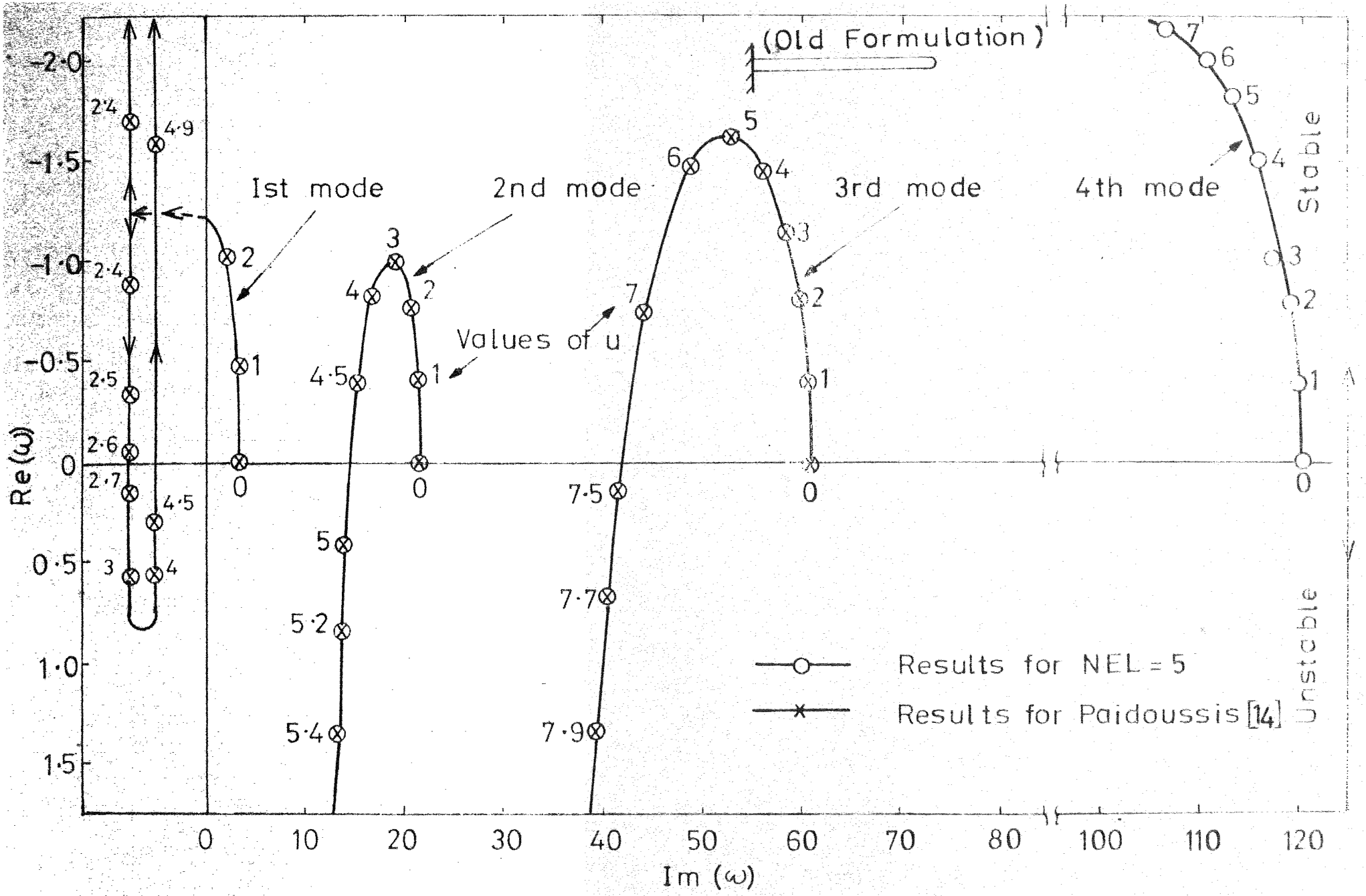

Fig. 3·9 The dimensionless complex frequency of clamped free rod with a tapered free end as a function of the dimensionless flow velocity u, for $\beta = 0{\cdot}5, \varepsilon c_f = 1, \delta = 0, Cm = 1, f_c = 0{\cdot}8, x_e/L = 0{\cdot}01$, NEL = 5

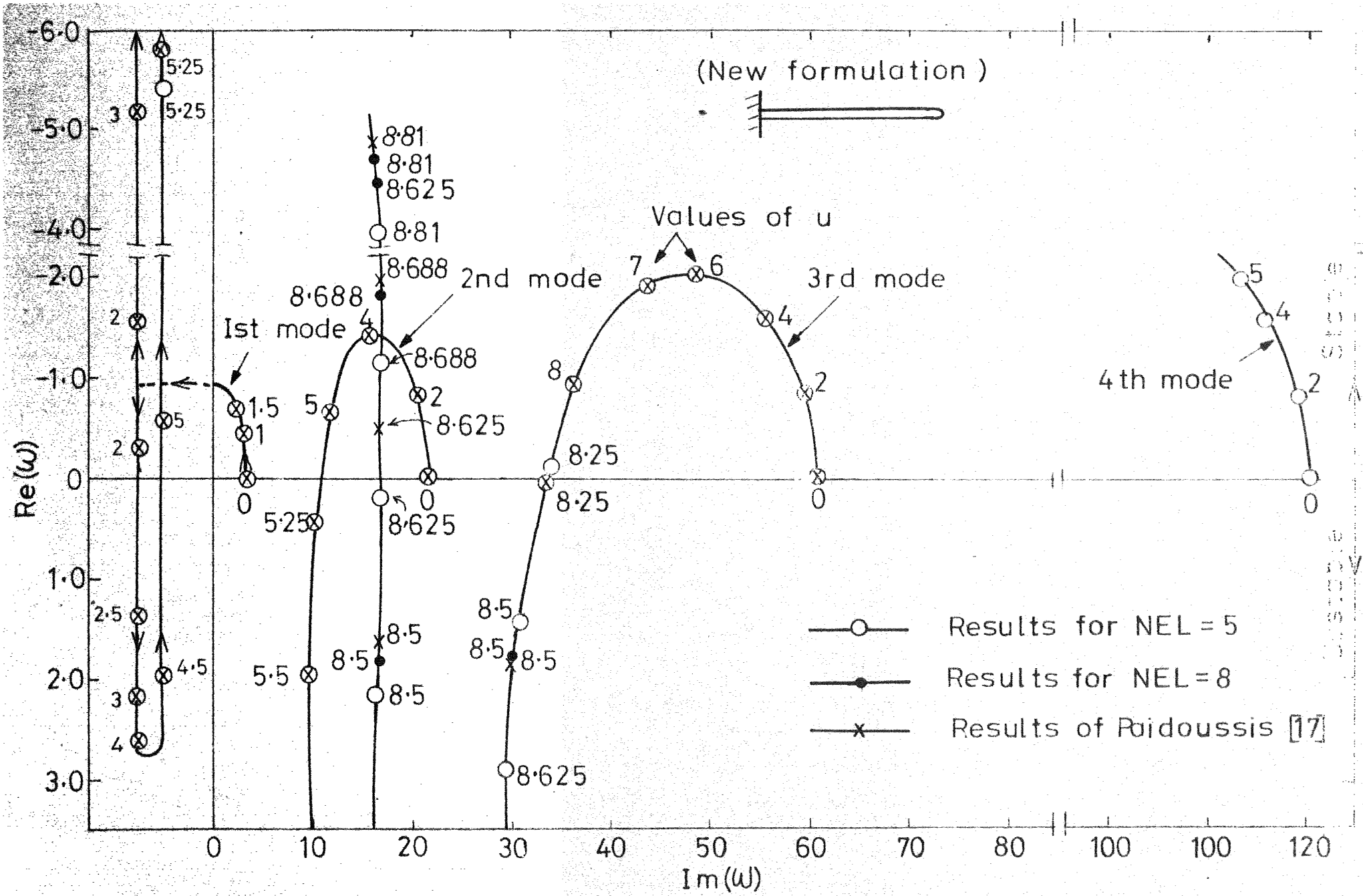

Fig.3·10 The dimensionless complex frequency of an isolated cantilever rod with a tapered free end as a function of the dimensionless flow velocity u, for $\beta = 0{\cdot}5$, $\varepsilon c_s = 1$, $\delta = 0$, $Cm = 1$, $f_c = 0{\cdot}8$, $x_e/L = 0{\cdot}01$, $c_L = \gamma = 0$, NEL = 5

REFERENCES

1. Benjamin, T.B., "Dynamics of a System of Articulated Pipes Conveying Fluid", Parts I and II, Proceedings of the Royal Society of London, Vol. 261, series A, 1961, pp. 457-499.

2. Burgreen, D., Byrnes , J.J., Benforado, D.M., "Vibration of Rods Induced by Water in Parallel Flow", Transactions of ASME, Vol. 80(5), 1958, pp. 991-1003.

3. Chen, S.S., Wambsganss, M. W., Jr., "Parallel Flow-Induced Vibration of Fuel Rods", Nuclear Engineering & Design, Vol.18, 1972, pp. 253-278.

4. Chen, S.S., "Parallel Flow-Induced Vibrations and Instabilities of Cylindrical Structures", The Shock and Vibration Digest, Vol. 6, No. 10, 1974, pp. 1-11.

5. Desai, C.S. and Abel, J.F., "Introduction to Finite Element Method", Van Nostrand Reinhold Co., New York, 1972.

6. Frazer, R.A., Duncan, W.J.and Collar, A.R., "Elementary Matrices", Cambridge University Press, New York, 1957, p. 327.

7. Howthorne, W.R., "The Early Development of the Dracone Flexible Barge", Proceedings of the Institution of Mechanical Engineers, Vol. 175, 1961, pp. 52-83.

8. Hoerner, S.F., "Fluid Dynamic Drag", 2nd edition, Brick town, N.J.: Hoerner Fluid Dynamics, 1965.

9. Huebner, K.H., "The Finite Element Method for Engineers", John Wiley and Sons, 1975.

10. Lighthill, M.J., "Note on the Swimming of Slender Fish", Journal of Fluid Mechanics, Vol. 9, 1960, pp. 305-317.

11. Meirovitch, L., "Analytical Methods in Vibrations", The Macmillan Company, London, 1967, p. 410.

12. Paidoussis, M.P., "The Amplitude of Fluid Induced Vibration of Cylinders in Axial Flow", Report AECL-2225, 1965, Atomic Energy of Canada Ltd., Chalk River, Ontario, Canada.

13. Paidoussis, M.P., "Vibration of Flexible Cylinders with Supported Ends Induced by Axial Flow", Institute of Mechanical Engineers Proceedings, Vol. 180, 1966, Part 3-J.

14. Paidoussis, M.P., "Vibration of Flexible Slender Cylinders in Axial Flow", Parts I and II, Journal of Fluid Mechanics, Vol. 26, 1966, pp. 717-751.

15. Paidoussis, M.P., Sharp, F.L., "An Experimental Study of the Vibrations of Flexible Cylinders Induced by Nominally Axial Flow", Report CRNL-76, 1967,Chalk River National Lab., Chalk River, Ontario, Canada.

16. Paidoussis, M.P., "Stability of Towed, Totally Submerged Flexible Cylinders", Journal of Fluid Mechanics, Vol. 34, 1968, pp. 273-297.

17. Paidoussis, M.P., "Dynamics of Cylindrical Structures Subjected to Axial Flow", Journal of Sound and Vibration, Vol. 29 (3),1973, pp. 365-385.

18. Paidoussis, M.P., "Vibration of Cylindrical Structures Induced by Axial Flow", Journal of Engineering for Industry, Transactions of ASME, Vol. 96, B, 1974, pp. 547-552.

19. Paidoussis, M.P., "The Dynamic Behavior of Cylindrical Structures in Parallel Flow", Annals of Nuclear Science and Engineering, Vol. 1, 1974, pp. 83-106.

20. Paidoussis, M.P., "Stability of Slender Cylinders in Pulsatile Axial Flow", Journal of Sound and Vibration, Vol. 42, 1975, pp. 1-11.

21. Pavlica, R.T., Marshall, R.C., "Vibration of Fuel Assemblies in Parallel Flows", Transactions of American Nuclear Society, Vol. 8, 1965, pp. 599-600.

22. Pavlica, R.T., Marshall, R.C., "An Experimental Study of Fuel Assembly Vibrations Induced by Coolant Flow", Nuclear Engineering and Design, Vol. 4, 1966, pp. 54-60.

23. Ralston, A., "A First Course in Numerical Analysis", McGraw Hill Book Company, New York, 1965, pp. 464-520.

24. Szabo, B.A., Lee, G.C., "Stiffness Matrix for Plates by Galerkin's Method", Journal of Engineering Mechanics Division, Vol. 95, No. 1-6, 1969, pp. 571-586.

25. Taylor, G.I., "Analysis of Swimming of Long and Narrow Animals", Proceedings of Royal Society of London, Vol. 214, series A, 1952, pp.158-183.

26. Deb. J.K., "Dynamic Stability of Pipes Conveying Fluid by Finite Element Method", M. Tech. Thesis, Mech. Engg. Deptt., IIT, Kanpur, April 1978.

27. Paidoussis, M.P., Issid, N.T., "Dynamic Stability of Pipes Conveying Fluid", Journal of Sound and Vibration, Vol. 33(3), 1974, pp. 267-294.

APPENDIX A

EQUATION OF SMALL LATERAL MOTIONS

The system to be considered for the present study consists of a flexible cylindrical rod which has circular cross-section. The rod is immersed in a fluid which is flowing with a uniform velocity V, parallel to the neutral axis of position of rest of the rod which coincides with the x-axis of the co-ordinate system considered as shown in Fig. (2-a). Cross-sectional area of the rod is A, linear density (mass per unit length) is m_r , with flexural rigidity EI, and total length of the rod is L. The density of the flowing fluid is ρ_f.

For the formulation, following idealizations are made:

(i) The rod is assumed to represent a Bernoulli-Euler beam.

(ii) The fluid flowing past the rod is considered to be incompressible.

(iii) Small lateral motions of the rod about its position of rest are considered, during which the angle of incidence $\bar{\theta}$ and $\frac{\partial \bar{\theta}}{\partial x}$ remain sufficiently small so that :

(a) no separation occurs in cross-flow,

(b) the fluid forces on each element of the rod may be assumed to be the same as those acting on a corresponding element of a long straight rod of the same

cross-sectional area and inclination.

(iv) The fluid is supposed to be contained by boundaries sufficiently distant from the rod to have negligible influence on its motion. This assumption is made for the system which consists of a rod immersed in an infinite fluid and is not valid for arod-shell system.

(v) The virtual mass is equal to $\rho_r A$ for unconfined flow, where ρ_r is the density of the material of the circular rod; and otherwise $C_m \rho_r A$, where C_m is coefficient of virtual mass, Paidoussis [17] and Chen [3].

(vi) The fluid flow is steady and uniform.

(vii) The rod is supported at one or both of its extremities, and it is assumed that the supports are such that they generate, at most, only localized disturbances to the idealized flow conditions assumed here.

A.1 FORCES TO BE CONSIDERED :

We now consider a small element δx of the rod, as shown in Fig. (2.a), where T is the tension, Q is the shear force, M is the bending moment, $m_r(\partial^2 y/\partial t^2)\,\delta x$ is the inertia force of the rod. F_N and F_L are the frictional forces per unit length in the transverse and longitudinal directions, respectively, and $m_r g$ is the rod gravity. Apart from these forces the rod is subjected to fluid pressures and hydrodynamic force which will be discussed in

detail along with the frictional forces in the next section.

A.1.1 FLUID PRESSURE :

Let F_{px} and F_{py} be the resultants of the steady-state pressure p acting on the outer surface of the element. These resultants can be found as follows : Consider the element δx of Fig. (2-a), momentarily frozen and immersed in fluid on all sides as in Fig. (2-b); then there will be forces pA and $pA + \frac{\partial (pA)}{\partial x}$, on the two forces of the element in addition with F_{px} and F_{py}. The resultant of these additional forces and of $F_{px}\ \delta x$ and $F_{py}\ \delta x$ is equal to the buoyancy force. Assuming $p \equiv p(x)$ is a linear function of x (which is reasonable to assume, as it applies to both a hydrostatic pressure distribution and to one modified by skin friction pressure drop), it can be written (see Fig. (2-b))

$$\Sigma F_x = 0 \Longrightarrow - F_{px}\ \delta x - \left(pA + \frac{\partial (pA)}{\partial x}\ \delta x\right) + pA$$

$$= \text{buoyancy force}$$

$$= - \frac{\partial p}{\partial x}\ A\ \delta x$$

and

$$\Sigma F_y = 0 \Longrightarrow F_{py}\ \delta x - \left(pA + \frac{\partial (pA)}{\partial x}\right)\left(\frac{\partial y}{\partial x} + \frac{\partial^2 y}{\partial x^2}\ \delta x\right)$$

$$+ pA \frac{\partial y}{\partial x} = 0 ,$$

hence neglecting the higher order terms, one obtains

$$\begin{aligned} - F_{px} &= - \frac{\partial p}{\partial x}\ A + \frac{\partial (pA)}{\partial x} , \\ F_{py} &= \frac{\partial}{\partial x}\left(pA \frac{\partial y}{\partial x}\right) . \end{aligned} \qquad \text{(A-1)}$$

Thus, from Eqn. (A-1) it is obvious that F_{py} is equivalent to a tensile force, acting at the cross-section of the rod, of magnitude pA. Also, if $\frac{\partial A}{\partial x} = 0$, $F_{px} = 0$, hence for a rod of uniform cross-section, the only pressure force acting on the element is equivalent to a tensile force equal to F_{py}.

A.1.2 HYDRODYNAMIC FORCE :

The inviscid hydrodynamic force F_A, which is equal to the lateral force per unit length acting on the rod, and is given by the change in momentum of the lateral flow about the rod, Lighthill [10].

The components of fluid velocity in x- and y-directions are, respectively,

$$V_x = V \cos \bar{\theta} ,$$

$$V_y = V \sin \bar{\theta} , \qquad (A-2)$$

where $\bar{\theta}$ is the angle between the axis of rod and the flow direction.

Assuming small transverse motions of the rod in either direction of its axis, $\bar{\theta}$ may be approximated by

$$\bar{\theta} = (1/V) [(\partial y/\partial t) + V (\partial y/\partial x)] . \qquad (A-3)$$

Therefore, from Eqns. (A-2) and (A-3) one obtains

$$V_x = V \text{ as } \cos \bar{\theta} = 1 ,$$

and $$V_y = [(\partial y/\partial t) + V (\partial y/\partial x)] . \qquad (A-4)$$

Momentum of the lateral flow of the fluid is

$$C_m m_f [(\partial y/\partial t) + V (\partial y/\partial x)] ,$$

hence the rate of change of momentum per unit length becomes

$$(\partial / \partial t + V \partial / \partial x) [C_m m_f (\partial y/\partial t + V \partial y/\partial x)], \quad (A-5)$$

where m_f is the virtual mass per unit length of the rod, which is given by

$$m_f = \frac{\pi D^2}{4} \rho_f , \quad (A-6)$$

where D is the rod diameter, ρ_f is the fluid density. C_m is a "virtual mass" coefficient which is discussed by Chen [3] in detail.

According to Lighthill [10], the rate of change of momentum per unit length gives rise to an equal and opposite lateral force on the rod, i.e.,

$$F_A = C_m m_f [\partial / \partial t + V \partial / \partial x]^2 y. \quad (A-7)$$

A.1.3 FRICTIONAL FORCES :

Friction forces acting on a rough cylinder set obliquely to a fluid stream are taken as proposed by Taylor [25]. For rough cylinders, he suggested the following expressions for normal and tangential drag forces :

$$F_N = \frac{1}{2} \rho_f D V^2 (C_f \sin \bar{\theta} + C_{DP} \sin^2 \bar{\theta}), \quad (A-8)$$

$$F_L = \frac{1}{2} \rho_f D V^2 C_f \cos \bar{\theta}, \quad (A-9)$$

where $\bar{\theta}$ is the angle between the axis of cylinder and flow direction and C_f and C_{DP} are drag coefficients associated with skin friction and pressure, respectively. Hoerner's [8] expressions

of viscous forces also reduce to Eqns. (A-8) and (A-9), Paidoussis [17] .

For small oscillations, as mentioned previously, the angle of incidence $\bar{\theta}$ can be approximated by Eqn. (A-3),

$$\bar{\theta} = (1/V) \left[(\partial y/\partial t) + V (\partial y/\partial x) \right],$$

hence Eqns. (A-8) and (A-9) reduce to

$$F_N = \frac{1}{2} \rho_f D V C_f \left(\frac{\partial y}{\partial t} + V \frac{\partial y}{\partial x}\right),$$

and $$F_L = \frac{1}{2} \rho_f D V^2 C_f . \qquad \text{(A-10)}$$

A.1.4 VISCOUS-DAMPING FORCE :

The force representing the viscous damping effect can be expressed as, Paidoussis [17] ,

$$F_D = \frac{1}{2} \rho_f D C_D \frac{\partial y}{\partial t}$$

Therefore, Eqns. (A-10) may be written as

$$F_N = \frac{1}{2} \rho_f D V C_f \left(\frac{\partial y}{\partial t} + V \frac{\partial y}{\partial x}\right) + \frac{1}{2} \rho_f D C_D \frac{\partial y}{\partial t} ,$$

$$F_L = \frac{1}{2} \rho_f D V^2 C_f . \qquad \text{(A-11)}$$

A.2 EQUATION OF MOTION :

The forces and moments acting on a small element, δx , of the rod, which has undergone a small lateral displacement $y(x,t)$ have been determined and are shown in Fig. (2.a). The force balances in the x- and y-directions, and a moment balance, Paidoussis [17] are

$$\frac{\partial T}{\partial x} + m_r g + F_L + (F_N + F_A)\frac{\partial y}{\partial x} - F_{px} = 0 , \qquad (A-12)$$

$$\frac{\partial Q}{\partial x} - F_N - F_A + F_{py} + F_L\frac{\partial y}{\partial x} + \frac{\partial}{\partial x}\left(T\frac{\partial y}{\partial x}\right) - m_r\frac{\partial^2 y}{\partial t^2} = 0,$$

..... (A-13)

$$Q = -\frac{\partial M}{\partial x} = -\frac{\partial}{\partial x}\left(EI\frac{\partial^2 y}{\partial x^2}\right) - \mu\frac{\partial}{\partial x}\left(I\frac{\partial^3 y}{\partial x^2\,\partial t}\right), \qquad (A-14)$$

where the fact that y and its derivatives are small has been utilized, and it has been assumed that Euler - Bernoulli beam theory is adequate to describe the motions of the rod; moreover, a Kelvin-Voigt type of damping in the material of the rod has been assumed to apply.

Substituting Eqns. (A-1) into Eqns. (A-12) and (A-13), one obtains

$$\frac{\partial}{\partial x}(T + pA) + \left(m_r g - \frac{\partial p}{\partial x}A\right) + F_L + (F_N + F_A)\frac{\partial y}{\partial x} = 0,$$

... (A-15)

$$\frac{\partial Q}{\partial x} - F_N - F_A + F_L\frac{\partial y}{\partial x} + \frac{\partial}{\partial x}\left\{(T + pA)\frac{\partial y}{\partial x}\right\} - m_r\frac{\partial^2 y}{\partial t^2} = 0.$$

... (A-16)

Now, if $y \sim O(\epsilon)$, then F_N and F_A are of the same order , Paidoussis [17], so that

$$(F_A + F_N)\,(\partial y/\partial x) \sim O(\epsilon^2),$$

neglecting these terms in Eqn. (A-15) and integrating it from x to L, upon combining it with Eqns. (A-15), (A-16) and (A-14), one obtains

$$\mu I \frac{\partial^5 y}{\partial x^4 \partial t} + EI \frac{\partial^4 y}{\partial x^4} + F_A - \left[(T + pA)_L + m_r g (L - x) \right.$$

$$\left. - \frac{\partial p}{\partial x} A (L - x) + \int_x^L F_L \, dx \right] \frac{\partial^2 y}{\partial x^2} + F_N + (m_r g - \frac{\partial p}{\partial x} A)$$

$$\frac{\partial y}{\partial x} + m_r \frac{\partial^2 y}{\partial t^2} = 0. \qquad (A-17)$$

The terms F_A, F_N and F_L have already been determined in sections A.1.2 and A.1.3. Now the terms $(T + pA)_L$ and $\frac{\partial p}{\partial x}$ will be determined considering the case of an isolated rod in parallel flow.

A.2.1 CASE OF AN ISOLATED ROD IN PARALLEL FLOW :

When the cylinder is isolated in a fairly large flow channel the pressure drop due to flow may be considered to be negligible, and

$$\frac{\partial p}{\partial x} = \rho_f g \, . \qquad (A-18)$$

Considering the term $(T + pA)_L$, if the rod is free to slide axially (or is free completely), at $x = L$, one obtains $T_L = - p_b A$ (since pA arises from the pressure on the sides of the rod), where p_b is the base pressure; hence $(T + pA)_L = (p_L - p_b) A$. Since $p_b < p_L$ generally, this represents, more or less, "form" drag, more accurately referred to as base drag, which may be expressed as

$$(T + pA)_L = \frac{1}{2} \rho_f D^2 V^2 C_b . \qquad (A-19)$$

If the total length of the rod is fixed between fixed supports, at x = L there will be a compressive load $-\frac{1}{2}\rho_f D V^2 C_f (L/2)$ $-(m_r g - \frac{\partial p}{\partial x} A)\frac{L}{2}$, where the existence of the term $m_r g(L/2)$ depends on whether the length was fixed while the cylinder was horizontal or not. This fact can be explained as follows:

Eqn. (A-15) can be rewritten after rearranging and neglecting the higher order term as

$$\frac{\partial}{\partial x}(T + pA) = -(m_r g - \frac{\partial p}{\partial x} A) - F_L . \qquad (A-20)$$

Integrating Eqn. (A-20) between the limits x to L one obtains tensile force distribution along the whole length of the rod as

$$(T + pA)_x = (T + pA)_L + (m_r g - \frac{\partial p}{\partial x} A)(L - x) + F_L(L - x) .$$

..... (A-21)

Now the stress - strain relation gives the strain in the rod due to tensile forces

$$\frac{du_L}{dx} = \frac{1}{EA}(T + pA)_x , \qquad (A-22)$$

where u_L is change in the length of the rod.

Substituting Eqn. (A-22) in Eqn. (A-21) and integrating the resultant expression between 0 to L, one obtains

$$\int_0^L du_L = \frac{1}{EA}\int_0^L [(T + pA)_L + (m_r g - \frac{\partial p}{\partial x} A)(L - x)$$

$$+ F_L(L - x)]\, dx$$

$$\text{or} \quad 0 = \frac{1}{EA}\left[(T + pA)_L L + \left(m_r g - \frac{\partial p}{\partial x} A\right)\left(L^2 - \frac{L^2}{2}\right) + F_L\left(L^2 - \frac{L^2}{2}\right)\right]. \qquad (A\text{-}23)$$

since fixed length requirement implies that u_L must be equal to zero.

Solving Eqn. (A-23), one gets

$$(T + pA)_L = - F_L(L/2) - \left(m_r g - \frac{\partial p}{\partial x} A\right)(L/2)$$

$$= -\left[\frac{1}{2} \rho_f D V^2 C_f + m_r g - \frac{\partial p}{\partial x} A\right](L/2). \qquad (A\text{-}24)$$

Moreover, there will also be a compressive load due to radial contraction, for a thin tubular rod this is equal to $- 2\nu (\overline{pA})$. And there may also be an externally imposed uniform axial tension $\overline{T}$.

Therefore for this case

$$(T + pA)_L = -\left[\frac{1}{2} \rho_f D V^2 C_f + m_r g - \frac{\partial p}{\partial x} A\right](L/2)$$

$$+ (1 - 2\nu)(\overline{pA}) + \overline{T}. \qquad (A\text{-}25)$$

Combining Eqns. (A-19) and (A-25), and substituting into Eqn. (A-17) along with Eqns. (A-18), (A-7) and (A-11), one obtains the equation of small lateral motions

$$\mu I \frac{\partial^5 y}{\partial x^4 \partial t} + EI \frac{\partial^4 y}{\partial x^4} + C_m m_f \left(\frac{\partial}{\partial t} + V \frac{\partial}{\partial x} \right)^2 y$$

$$-\{\delta[\bar{T} + (1 - 2\nu)(\overline{pA})] + [\frac{1}{2} \rho_f D V^2 C_f + (m_r - m_f) g]$$

$$[(1 - \frac{1}{2}\delta) L - x] + \frac{1}{2} \rho_f D^2 V^2 (1 - \delta) C_L \} \frac{\partial^2 y}{\partial x^2} + \frac{1}{2} \rho_f D V C_f$$

$$\left(\frac{\partial y}{\partial t} + V \frac{\partial y}{\partial x} \right) + \frac{1}{2} \rho_f D C C_D \frac{\partial y}{\partial t} + (m_r - m_f) g \frac{\partial y}{\partial x} + m_r \frac{\partial^2 y}{\partial t^2} = 0, \quad \text{....} \quad (A\text{-}26)$$

where $\delta = 0$ signifies that the downstream end is free to slide axially, and $\delta = 1$ if the supports do not allow net axial tension.

APPENDIX B

EQUATION OF MOTION (OLD FORMULATION) AND IT'S FINITE ELEMENT ANALYSIS

Neglecting gravity, pressurization effects, internal damping and the y-component of tangential frictional force F_L , i.e., $F_L(\frac{\partial y}{\partial x})$ Eqn. (A-26) becomes

$$EI \frac{\partial^4 y}{\partial x^4} + C_m m_f (\frac{\partial}{\partial t} + V \frac{\partial}{\partial x})^2 y - \{\delta \bar{T} + [\frac{1}{2} \rho_f D V^2 C_f] [(1 - \delta/2) L - x]\} \frac{\partial^2 y}{\partial x^2} + \frac{1}{2} \rho_f D V C_f (\frac{\partial y}{\partial t} + V \frac{\partial y}{\partial x}) + \frac{1}{2} \rho_f D V^2 C_f \frac{\partial y}{\partial x} + m_r \frac{\partial^2 y}{\partial t^2} = 0 \qquad (B-1)$$

Eqn. (B-1) represents the equation used by Paidoussis[14] which has been referred as "Old Formulation" in the present work. It does not take into account the frictional forces correctly. Comparing this equation with Eqn. (A-26), one observes that in new formulation the term obtained by combining the coefficients of $x \frac{\partial^2 y}{\partial x^2}$ and $\frac{\partial y}{\partial x}$ is $F_L (x \frac{\partial^2 y}{\partial x^2} + \frac{\partial y}{\partial x})$ (neglecting gravity) and in the old formulation the above term becomes $F_L(x \frac{\partial^2 y}{\partial x^2} + 2\frac{\partial y}{\partial x})$. In the new formulation integration by parts of the above terms is straight forward, see Eqn. (2.13). Integration by parts of the corresponding

term for old formulation was not so straight forward. This difficulty was overcome by splitting this term and then integrating by parts as follows:

$$F_L \left(x \frac{\partial^2 y}{\partial x^2} + \frac{\partial y}{\partial x} \right) = F_L \left(x \frac{\partial^2 y}{\partial x^2} + \frac{\partial y}{\partial x} \right) + F_L \frac{\partial y}{\partial x} . \qquad \text{(B-2)}$$

Integration of all the terms of old formulation is given in Chapter 2, except of the term $F_L \frac{\partial y}{\partial x}$. Applying finite element based Galerkin's method, this term in Eqn. (B-2) turns out to be after integrating by parts

$$\int_0^h N_i F_L \frac{\partial y}{\partial x}^{(e)} dx = \left| N_i F_L y^{(e)} \right|_0^h - \int_0^h \frac{dN_i}{dx} F_L y^{(e)} dx . \qquad \text{(B-3)}$$

Substituting Eqn. (2.25) into Eqn. (B-3), one obtains for the element, e,

$$\begin{Bmatrix} \left| N_1 F_L y^{(e)} \right|_0^h \\ \vdots \\ \left| N_4 F_L y^{(e)} \right|_0^h \end{Bmatrix} - [k4]^{(e)} \{y\}^{ne} , \qquad \text{(B-4)}$$

where $[k4]^{(e)} = F_L \int_0^h \{N'\} \lfloor N \rfloor dx$

$$= F_L \begin{bmatrix} -1/2 & h/10 & 1/2 & -h/10 \\ -h/10 & 0 & h/10 & -h^2/60 \\ -1/2 & -h/10 & 1/2 & h/10 \\ h/10 & h^2/60 & -h/10 & 0 \end{bmatrix} , \qquad \text{(B-5)}$$

and the boundary condition to be considered becomes for the whole domain

$$\left\{\begin{array}{c} -1/2\ \rho_f D V^2 C_f y^{(e)}\Big|_1 \\ 0 \\ 0 \\ \vdots \\ 0 \\ +1/2\ \rho_f D V^2 C_f y^{(e)}\Big|_{m+1} \\ 0 \end{array}\right\} \qquad \text{(B-6)}$$

It should be noted that the values $-1/2\ \rho_f D V^2 C_f$ and $1/2\ \rho_f D V^2 C_f$ are summed up with $K_{1,1}$ and $K_{2m+1,2m+1}$ elements of the assembled stiffness matrix, respectively.

APPENDIX C

BOUNDARY CONDITIONS FOR A CANTILEVERED ROD WITH TAPERED FREE END

If the downstream end is free, terminating in a tapering end, the cross-sectional area of which varies smoothly from A to zero in a distance l ($<< L$), y and the lateral velocity v may be considered constant for the length l, Paidoussis [14] . This requirement allows the forces acting on the tapered end to be lumped and considered in appropriate boundary conditions, Hawthorne[7] . In the transverse direction equilibrium equation over the tapered end, say for $L - l < x < L$, is

$$\int_{L-l}^{L} \frac{\partial Q}{\partial x}\, dx - f_c \int_{L-l}^{L} \left(\frac{\partial}{\partial t} + V \frac{\partial}{\partial x} \right) [\, m_f(x)\, v \,]\, dx$$

$$- \int_{L-l}^{L} m_r(x)\, \frac{\partial^2 y}{\partial t^2}\, dx = 0 \qquad (C-1)$$

The parameter f_c , which is equal to unity for slender body, inviscid flow theory, has been introduced because the theoretical lateral force at the free end may not be fully realised as a result of (a) the lateral flow not being fully two-dimensional, since the fluid has opportunity to pass around rather than over the tapered end [Munk, M.M., 1924 NACA Rep. No. 184], and (b) boundary-layer effects, Hawthorne [7] . Accordingly f_c will normally be less

than unity, Paidoussis [14] .

Writing $m_f(x) = {}_f A(x)$ and $m_r(x) = {}_r A(x)$ and, since y and v are constant over the tapered end, Eqn. (C-1) leads to

$$\int_{L-l}^{L} \frac{\partial Q}{\partial x}\, dx - f_c\ \rho_f V v \int_{L-l}^{L} \frac{\partial A}{\partial x}\, dx - (\rho_r + f_c\ \rho_f) \frac{\partial^2 y}{\partial t^2} \int_{L-l}^{L} A(x)\, dx = 0 \qquad (C\text{-}2)$$

which yields

$$EI \frac{\partial^3 y}{\partial x^3} + \mu I \frac{\partial^4 y}{\partial x^3 \partial t} + f_c\ m_f V \left(\frac{\partial y}{\partial t} + V \frac{\partial y}{\partial x}\right) - (m_r + f_c\ m_f)\, xe \frac{\partial^2 y}{\partial t^2} = 0 , \qquad (C\text{-}3)$$

where

$$xe = \frac{1}{A} \int_{L-l}^{L} A(x)\, dx . \qquad (C\text{-}4)$$

Furthermore, it may be assumed that there is no bending moment at the free end, thus

$$EI \frac{\partial^2 y}{\partial x^2} + \mu I \frac{\partial^3 y}{\partial x^2 \partial t} = 0 . \qquad (C\text{-}5)$$

APPENDIX D

THE COMPUTER PROGRAM

The computer programme was prepared for assembling the system matrices, substituting the boundary conditions, inverting the assembled stiffness matrix, forming the dynamical matrix and finally for finding out the complex frequencies of the system.

The computer programme was written in Fortran IV and run on an IBM 7044 computer with approximately 32K words of core storage. The programme is quite general and built-in subroutines MATINV for matrix inversion and ZINDLA for finding out complex frequencies were called directly.

Fortran listing of the program is given in Appendix E.

D.1 DESCRIPTION OF PROGRAM :

The MAIN programme reads and prints various input data and output results. Other subroutines calculate the matrices, assemble them and after applying boundary conditions form the dynamical matrix. The complex eigenvalues are calculated by calling built-in subroutine ZINDLA.

Subroutine Name	Description
STIFF	Called by MAIN, calculates the various elemental stiffness matrices,

Subroutine Name	Description
	total stiffness matrix, assembles them, introduces bourdary conditions by calling BNDRY and calculates inverse by calling MATINV.
MASS	Called by MAIN, calculates the elemental mass matrix, assembles and introduces boundary conditions by calling ASMBL and BNDRY subroutines.
DAMP	Called by MAIN, calculates the elemental damping matrices, sums them up, assembles them and introduces boundary conditions by calling ASMBL and DNDRY subroutines in turn.
ASMBL	Called by MASS and DAMP, assembles the mass and damping matrices in turn.
BNDRY	Called by STIFF, MASS and DAMP, introduces boundary conditions to the assembled stiffness, mass and damping matrices and separates the required matrix.
MATMPY	Called by MAIN, forms the dynamical matrix.

Subroutine Name	Description
MATINV	Called by STIFF, computes matrix inverse.
EIGENP	Called by MAIN, determines eigenvalues and eigenvectors of a general real matrix. The binary version of this programme is stored on 1301 disk file, which is named ZINDIA (For further details refer to communication of ACM journal, Vol 2, 1968, pp. 820).

LIST OF PRINCIPIE VARIABLES

FORTRAN Implementation Program Symbol	Definition
MAIN PROGRAM	
AL	Length of the rod.
AMI	Moment of inertia of the rod.
AMF	Mass of fluid per unit length.
AMP	Mass of rod per unit length
AREA	Cross-sectional area of the rod
AV	Actual velocity of the fluid
BETA	Dimensionless mass of fluid
CBAR, CDASH	Friction drag coefficients.
CM	Coefficient of virtual mass.

FORTRAN Implementation Program Symbol	Definition
MAIN PROGRAM	
DO, DI	Outer and inner diameters of the rod, respectively.
E	Modulus of elasticity.
EVIN(I)	Imaginary part of dimensionless eigenvalue.
EVRN(I)	Real part of dimensionless eigenvalue.
FAC	Dividing factor which gives dimensionless eigenvalues.
FL	Tangential drag force.
I	Number of elements.
NMIN	Minimum number of elements.
NMAX	Maximum number of elements.
NSP	Total number of velocity points.
OMEGA1, OMEGA2, OMEGA3	Lowest three exact natural frequencies.
ROWF	Density of fluid.
ROWP	Density of rod.
VNON	Dimensionless velocity.
SVNON	Dimensionless velocity data.
SUBROUTINE STIFF	
AXP	Axial distance from upstream end to node p, see Fig. (1- c).

Program Symbol	Definition
SUBROUTINE STIFF	
ELMT	Length of one element.
FACTOR	Largest element of GSM
MAN	Factor multiplied to elemental stiffness matrix XNDND (4,4)
N	Size of the assembled matrix = 2 x (I+1)
N1	Size of the separated matrix
P	Factor multiplied to elemental beam stiffness matrix
GSB	Assembled stiffness matrix (N,N)
GSM	Separated stiffness matrix (N1,N1).
S	Total elemental stiffness matrix (4,4).
S1	Elemental beam stiffness matrix (4,4).
S2	Elemental stiffness matrix MFVSQ (4,4).
S3	Elemental stiffness matrix DY/DX (4,4).
S4	Elemental stiffness matrix XNDND (4,4).
S6	S1 + S3 - S4
X	Factor multiplied to matrix S3.
Z	Factor multiplied to matrix S2
SUBROUTINE MASS	
AM	Elemental mass matrix (4,4).
GMB	Assembled mass matrix (N,N).

Program Symbol	Definition
SUBROUTINE MASS	
GMM	Separated mass matrix (N1,N1).
N	Size of assembled mass matrix=2x(I+1)
P	Factor multiplied to matrix AM.
SUBROUTINE DAMP	
ALPHA	Factor multiplied to matrix C2
C	Elemental damping matrix AMPAV (4,4).
C1	Elemental damping matrix DY/DT (4,4).
C2	Elemental internal damping matrix (4,4).
C3	Total elemental damping matrix (4,4).
GCB	Assembled damping matrix (N,N).
CCM	Separated damping matrix (N1,N1).
N	Size of assembled damping matrix = 2 x (I + 1).
P	Factor multiplied to matrix C.
PINKI	Factor multiplied to matrix C1.
SUBROUTINE ASMBL	
AA	Elemental matrix (4,4).
ASM	Assembled matrix (N,N).
N	Total number of degree of freedom of the system (size of ASM)=2 x(I+1).

Program Symbol	Definition
SUBROUTINE BNDRY	
ASM	Assembled matrix (N,N).
BSM	Separated matrix (N1,N1)
N	Dimension of ASM = 2 x (I+1).
N1	Dimension of BSM.
SUBROUTINE MATMPY	
D	Unitary matrix I , (N1,N1)
D1	$[K^{-1} M]$, (N1,N1)
D2	$[K^{-1} C]$, (N1,N1)
DMM	Dynamical matrix (NB, NB).
N1	Dimension of $[K]^{-1}$, $[M]$, $[C]$, $[I]$ and $[O]$
NB	Dimension of dynamical matrix = 2xN1
SUBROUTINE MATINV	
A	Coefficient matrix of size N1 to be inversed.
B	Constant vector of size N1
M	Number of constant vectors (if M = 0, only inverse is computed).
DETERM	Value of the determinant
SUBROUTINE EIGENP	
A	Matrix of size N1 x N1 for which eigenvalues and eigenvectors are

Program Symbol

SUBROUTINE EIGENP

EVI (I)	Imaginary part of eigenvalue
EVR (I)	Real part of eigenvalue
NM	Dimension of dynamical matrix given in the main programme ($NM \geqslant N$)
T	Number of binary digits in the mantissa of a single precision floating point number = 27.0
VECI (J,I)	Imaginary part of eigenvector
VECR (J,I)	Real part of eigenvector

APPENDIX E

```
C*************************************************************
C  FINITE ELEMENT ANALYSIS OF DYNAMIC STABILITY OF CYLINDRICAL RODS
C  SUBJECTED TO PARALLEL FLOW.
C  CALLED BY------
C  PINNED--PINNED ROD, DECK NUMBER-1111111111111111.
C*************************************************************
C  PROGRAM SYMBOLS
C  ---------------
C  AL IS THE LENGTH OF THE ROD.
C  AMI IS THE MOMENT OF INERTIA OF THE ROD.
C  AMF IS THE MASS OF THE FLUID PER UNIT LENGTH.
C  AMP EXPRESSES THE VIRTUAL MASS OF THE ROD PER UNIT LENGTH.
C  AMP IS THE MASS OF THE ROD PER UNIT LENGTH.
C  AREA IS THE CROSS-SECTIONAL AREA OF THE ROD.
C  AV IS THE ACTUAL VELOCITY OF THE FLUID.
C  BETA IS THE DIMENSIONLESS MASS OF THE FLUID.
C  CBAR AND CDASH ARE THE FRICTIONAL DRAG COEFFICIENTS.
C  CM IS THE COEFFICIENT OF VIRTUAL MASS.
C  DO AND DI ARE THE OUTER AND INNER DIAMETERS OF THE ROD,RESPECTIVELY.
C  E IS THE MODULUS OF ELASTICITY OF THE MATERIAL OF THE ROD.
C  EVI(I) IS THE IMAGINARY PART OF DIMENSIONLESS EIGENVALUE.
C  EVR(I) IS THE REAL PART OF DIMENSIONLESS EIGENVALUE.
C  FAC IS THE DIVIDING FACTOR WHICH GIVES DIMENSIONLESS EIGENVALUES.
C  FL IS THE TANGENTIAL DRAG FORCE.
C  I IS THE NUMBER OF ELEMENTS.
C  IMIN IS THE MINIMUM NUMBER OF ELEMENTS.
C  IMAX IS THE MAXIMUM NUMBER OF ELEMENTS.
C  JSP IS THE TOTAL NUMBER OF VELOCITY POINTS.
C  OMEGA1,OMEGA2,OMEGA3 ARE THE LOWEST THREE EXACT NATURAL FREQUENCIES.
C  ROWF IS THE DENSITY OF THE FLUID.
C  ROWP IS THE DENSITY OF THE ROD.
C  VNOW IS THE DIMENSIONLESS FLOW VELOCITY.
C  SVNOW IS THE DIMENSIONLESS FLOW VELOCITY DATA.
C*************************************************************
      COMMON/B1/S(10,10)
      COMMON/B2/GSM(20,20)
      COMMON/B3/M(10,10)
      COMMON/B4/GMM(20,20)
      COMMON/B5/C(10,10)
      COMMON/B6/GCM(20,20)
      COMMON/B8/D2(20,20)
      COMMON/B9/D(20,20)
      COMMON/B11/AMF,AV
      COMMON/B12/AMI,E
      COMMON/B13/AF,AMP,FL
      COMMON/B14/AL
      COMMON/B15/RCWP,ROWF,AREA
      COMMON/B17/I,JJJ
      COMMON/B18/DMM(30,30)
      COMMON/B19/D1(20,20)
      COMMON/B20/CBAR,CDASH
      COMMON/B21/S1(10,10)
      COMMON/B22/C1(10,10)
      COMMON/B23/S2(10,10)
      COMMON/B24/C2(10,10)
      COMMON/B25/DO,DI
      COMMON/B26/S3(10,10)
      COMMON/B27/S4(10,10)
      DIMENSION SVNOW(15)
      CALL FLUN(20000)
      CALL FLOV(20000)
C*************************************************************
      REAL M,AMI,AL
      DATA  CM/1.0/
      DATA   DO,DI/0.0127,0.009534/
```

```
      AMI=(3.14*((DO**4)-(DI**4)))/64.
      AREA=(3.14*((DO**2)-(DI**2)))/4.
      AL/1.27/
      =0.1[illegible]+12
      DATA CBAR,CDASH/0.019625,0.0/
      DATA RHOP/7978.4/
      AMP=RHOP*3.14*((DO**2)/4.-(DI**2)/4.)
      DATA BETA/.1/
      PRINT100,CBAR,CDASH,BETA
  100 FORMAT(5X,*CBAR=*,E16.8,5X,*CDASH=*,E16.8,5X,*BETA=*,E16.8)
      AMF=(BETA*AMP)/(1.0-BETA)
      CMF=(4.*AMF)/(3.14*(DO**2))
      FAC=SQRT((E*AMI)/((AMF*CM+AMP)*(AL**4)))
      PRINT125,AMI,AMP,AMF,FAC,AREA
  125 FORMAT(5X,*AMI=*,5X,E16.8,5X,*AMP=*,E16.8,5X,*AMF=*,E16.8,5X,*FAC=
     1*,E16.8,5X,*AREA=*,E16.8)
      OMEGA1=9.87*FAC
      OMEGA2=39.5*FAC
      OMEGA3=88.9*FAC
      PRINT126,OMEGA1,OMEGA2,OMEGA3
  126 FORMAT(/,5X,*OMEGA1=*,E16.8,5X,*OMEGA2=*,E16.8,5X,*OMEGA3=*,E16.8)
      AL=ALSA
      DATA SVNON/0.0,1.0,2.0,3.0,4.0,5.0,6.0,7.0,8.0,9.0,10.0,11.0,12.0
     *,13.0,14.0/
      NSP=15
C     ******************************************************************
      NMIN=5
      NMAX=9
      DO 10 I=NMIN,NMAX
      VNON=0.0
      DO 20 JJJ=1,NSP
      VNON=SVNON(JJJ)
      AV=(SQRT((E*AMI)/AMF)*VNON)/AL
      FL=(RHOF*CD*(AV**2)*CBAR)/2.
      PRINT27,I,VNON,AV,FL
   27 FORMAT(/,5X,*I=*,I3,5X,*VNON=*,E16.8,5X,*AV=*,E16.8,5X,*FL=*,E16.8
     1)
      CALL STIFF
      CALL MASS
      CALL DAMP
      CALL MATMPY
      DIMENSION EVR(30),EVI(30),VECR(30,30),VECI(30,30),INDIC(30)
      DIMENSION EVRN(30),EVIN(30)
      T=27.0
      N1=(2*(I+1)-2)
      N=2*N1
      NM=30
      CALL EIGENP(N,NM,DMM,T,EVR,EVI,VECR,VECI,INDIC)
      DO 90 L=1,N
      DENOM=((EVR(L)**2)+(EVI(L)**2))
      EVR(L)=EVR(L)/DENOM
      EVI(L)=-EVI(L)/DENOM
      EVRN(L)=EVR(L)/FAC
      EVIN(L)=EVI(L)/FAC
   90 CONTINUE
      WRITE(6,33)
   33 FORMAT(/,17X,*EVR*,17X,*EVI*,20X,*EVRN*,17X,*EVIN*)
      PRINT34,(EVR(L),EVI(L),EVRN(L),EVIN(L),L=1,10)
   34 FORMAT(10X,E16.8,5X,E16.8,8X,E16.8,5X,E16.8)
      WRITE(6,35)
   35 FORMAT(/,2X,125(1H-))
      VNON=VNON+1.0
   20 CONTINUE
      WRITE(6,36)
   36 FORMAT(/,2X,125(1H*))
   10 CONTINUE
      STOP
      END
```

```
C     ******************************************************************
      SUBROUTINE STIFF
C     ******************************************************************
C     A(R) IS THE AXIAL CO-ORDINATE OF THE ELEMENT.
C     ELMT IS THE LENGTH OF ONE ELEMENT.
C     BIGGEST IS THE LARGEST ELEMENT OF MATRIX GSM.
C     GSM IS THE TOTAL ELEMENTAL STIFFNESS MATRIX.
C     GSB IS THE ELEMENTAL BEAM STIFFNESS MATRIX.
C     GMB IS THE ELEMENTAL STIFFNESS MATRIX MFVSQ.
C     GCB IS THE ELEMENTAL STIFFNESS MATRIX DY/DX.
C     S1 IS THE ELEMENTAL STIFFNESS MATRIX XNDAD.
C     GSM IS THE ASSEMBLED STIFFNESS MATRIX.
C     GSM IS THE SEPERATED STIFFNESS MATRIX.
      COMMON /B1/S(10,10)
      COMMON /B2/GSM(20,20)
      COMMON /B11/AMF,AMP
      COMMON /B12/AMI,E
      COMMON /B13/AF,AMP,FL
      COMMON /B14/AL
      COMMON /B17/I,JJJ
      COMMON /B21/S1(10,10)
      COMMON /B22/S2(10,10)
      COMMON /B25/DC,DI
      COMMON /B26/S3(10,10)
      COMMON /B27/S4(10,10)
      DIMENSION S6(4,4),GSB(20,20),GMB(20,20),GCB(20,20)
      DIMENSION P(20,1)
      DIMENSION AA(10,10),ASM(20,20),BSM(20,20)
      REAL ELMT,AL,AMI
C     ******************************************************************
      DATA CM,DELTA/1.0,1.0/
      DATA CB/0.0/
      GAMA=10.0
      G=(GAMA*E*AMI)/((AL**3)*(AMP-AMF))
      PRINT154,GAMA,G
  154 FORMAT(/,5X,*GAMA=*,E16.8,5X,*G=*,E16.8)
C     ******************************************************************
      CGAMA=0.0
      TBAR=(CGAMA*E*AMI)/(AL**2)
      PRINT155,CGAMA,TBAR
  155 FORMAT(5X,*CGAMA=*,E16.8,10X,*TBAR=*,E16.8)
+     ******************************************************************
      DATA ETA,NU/0.0,0.3/
      PABAR=(ETA*E*AMI)/(AL**2)
      PRINT156,ETA,NU,PABAR
  156 FORMAT(5X,*ETA=*,E16.8,5X,*NU=*,E16.8,5X,*PABAR=*,E16.8)
+     ******************************************************************
      ELMT=AL/FLOAT(I)
C     ******************************************************************
      P=(E*MI)/(ELMT**3)
      S(1,1)=12.*P
      S(1,2)=6.*ELMT*P
      S(1,3)=-S(1,1)
      S(1,4)=S(1,2)
      S(2,2)=4.*(ELMT**2)*P
      S(2,3)=-S(1,2)
      S(2,4)=2.*(ELMT**2)*P
      S(3,3)=S(1,1)
      S(3,4)=-S(1,2)
      S(4,4)=S(2,2)
      DO 1 IL=1,4
      DO 1 JL=1,4
    1 S(JL,IL)=S(IL,JL)
      IF(I.NE.2.OR.JJJ.GE.3) GO TO 78
      PRINT 101
  101 FORMAT(/,5X,*BEAM STIFFNESS MATRIX IS*)
      PRINT36,((S(II,JL),JL=1,4),II=1,4)
   36 FORMAT(/,4X,4E20.8)
   78 CONTINUE
+     ******************************************************************
```

```
      REAL   M
      W=FL+(AMP-AMF)*C
      REAL   MAN
      MAN=W/3.
      S4(1,1)=16.*MAN
      S4(1,2)=2.*ELMT*MAN
      S4(1,3)=-S4(1,1)
      S4(1,4)=0.0
      S4(2,2)=(ELMT**2)*MAN
      S4(2,3)=-S4(1,2)
      S4(2,4)=-(ELMT**2)/2.*MAN
      S4(3,3)=S4(1,1)
      S4(3,4)=0.0
      S4(4,4)=8.*(ELMT**2)*MAN
      DO 98 IK=1,4
      DO 98 JK=1,4
   98 S4(JK,IK)=S4(IK,JK)
      IF(I.NE.2.OR.JJJ.GE.3) GO TO 80
      PRINT 103
  103 FORMAT(/,5X,*STIFFNESS MATRIX XNONO IS*)
      PRINT22,((S4(IK,JK),JK=1,4),IK=1,4)
   22 FORMAT(/,4X,4E20.8)
   80 CONTINUE
     +*****************************************************************
      C=0.0
      S1(1,1)=-0.5*X
      S1(1,2)=(ELMT*X)/10.
      S1(1,3)=0.5*X
      S1(1,4)=-S1(1,2)
      S1(2,1)=-S1(1,2)
      S1(2,2)=0.0
      S1(2,3)=S1(1,2)
      S1(2,4)=-(X*(ELMT**2))/60.
      S1(3,1)=-0.5*X
      S1(3,2)=-S1(1,2)
      S1(3,3)=-S1(1,1)
      S1(3,4)=S1(1,2)
      S1(4,1)=S1(1,2)
      S1(4,2)=-S1(2,4)
      S1(4,3)=-S1(1,2)
      S1(4,4)=0.0
      IF(I.NE.2.OR.JJJ.GE.3) GO TO 81
      PRINT 104
  104 FORMAT(/,5X,*STIFFNESS MATRIX DY/DX IS*)
      PRINT23,((S1(IK,JK),JK=1,4),IK=1,4)
   23 FORMAT(/,4X,4E20.8)
   81 CONTINUE
     +*****************************************************************
      N=2*(I+1)
      DO  5  IL=1,4
      DO  5  JL=1,4
      S6(IL,JL)=0.0
      S6(IL,JL)=S6(IL,JL)+(S(IL,JL)+S1(IL,JL)-S4(IL,JL))
    5 CONTINUE
      DO 121  IK=1,N
      DO 121  JK=1,N
  121 GSB(IK,JK)=0.0
      AXP=0.0
      DO 122 K=1,I
      ZZ=(CM*AMF*(AV**2)-(DELTA*(TBAR+(1.0-2.0*NU)*(PABAR))+W*((1.0-0.5*
     1NU)*(PABAR))+W*((1.0-0.5*DELTA)*AL)+(0.5*ROWF*(DO**2)*(AV**2)*CB(1
     11.0-DELTA))))
      Z=(ZZ+W*AXP)/(30.0*ELMT)
      AXP=AXP+ELMT
      S2(1,1)=36.*Z
      S2(1,2)=3.*ELMT*Z
      S2(1,3)=-S2(1,1)
      S2(1,4)=S2(1,2)
      S2(2,2)=4.*(ELMT**2)*Z
      S2(2,3)=-S2(1,2)
```

```
      S2(3,4)=-(GLNT**2)*Z
      S2(4,3)=S2(3,4)
      S2(3,4)=-S2(1,2)
      S2(4,4)=S2(2,2)
      DO 1  IK=1,4
      DO 1  JK=1,4
    1 S2(JK,IK)=S2(IK,JK)
      IF(I.NE.2.OR.JJJ.GE.3) GO TO 79
      PRINT 12
   12 FORMAT(/,5X,*STIFFNESS MATRIX MFVSQ IS*)
      PRINT 23,((S2(IK,JK),JK=1,4),IK=1,4)
   23 FORMAT(/,4X,4E20.8)
   79 CONTINUE
      DO 41  IK=1,4
      DO 41  JK=1,4
      S3(IK,JK)=S4(IK,JK)-S2(IK,JK)
   41 CONTINUE
      IF(I.NE.2.OR.JJJ.GE.3) GO TO 82
      PRINT 25
   25 FORMAT(/,5X,*TOTAL STIFFNESS MATRIX IS*)
      PRINT24,((S3(IK,JK),JK=1,4),IK=1,4)
   24 FORMAT(/,4X,4E20.8)
   82 CONTINUE
      II=2*K-1
      JJ=II
      II3=II+3
      JJ3=JJ+3
      DO 122 IK=II,II3
      DO 122 JK=JJ,JJ3
      L=IK-II+1
      LJ=JK-JJ+1
      GSB(IK,JK)=GSB(IK,JK)+S3(L,LJ)
  122 CONTINUE
      CALL BNDRY(GSB,GSM)
     +*****************************************************************
      N=(2*(I+1)-2)
      FACTOR=ABS(GSM(1,1))
      DO 9  IK=1,N
      DO 9  JK=1,N
      IF(ABS(GSM(IK,JK)).GT.FACTOR) FACTOR=ABS(GSM(IK,JK))
    9 CONTINUE
      IF(I.NE.2.OR.JJJ.GE.3) GO TO 83
      PRINT37,FACTOR
   37 FORMAT(5X,*FACTOR=*,E16.8)
   83 CONTINUE
      DO 13 IK=1,N
      DO 13 JK=1,N
      GSM(IK,JK)=GSM(IK,JK)/FACTOR
   13 CONTINUE
      IF(I.NE.2.OR.JJJ.GE.3) GO TO 84
      PRINT 106
  106 FORMAT(/,5X,*ASSEMBLED STIFFNESS/FACTOR IS*)
      PRINT38,((GSM(IK,JK),JK=1,N),IK=1,N)
   38 FORMAT(/,5X,6E15.8)
   84 CONTINUE
C     CALLING  SUBROUTINE MATINV.
      N=(2*(I+1)-2)
      DO 30 II=1,N
   30 B(II,1)=0.0
      CALL MATINV(GSM,N,B,0,DETERM)
      IF(I.NE.2.OR.JJJ.GE.3) GO TO 85
      PRINT 107
  107 FORMAT(/,5X,*INVERSE OF GSM IS*)
      PRINT39,((GSM(IK,JK),JK=1,N),IK=1,N)
   39 FORMAT(/,5X,6E15.8)
   85 CONTINUE
      N=(2*(I+1)-2)
      DO 11 KI=1,N
      DO 11 KJ=1,N
      GSM(KI,KJ)=GSM(KI,KJ)/FACTOR
```

```
      CALL INVS
      IF(I.NE.2.OR.JJJ.GE.3) GO TO 86
      PRINT 109
  109 FORMAT(/,5X,*INVERSE OF GSM/FACTOR IS*)
      PRINT 77,((GSM(KI,KJ),KJ=1,N),KI=1,N)
   77 FORMAT(/,2X,4E20.8)
   86 CONTINUE
      RETURN
      END


C     ******************************************************************
      SUBROUTINE MASS
C     ******************************************************************
CC    AM IS THE ELEMENTAL MASS MATRIX.
CC    AMB IS THE ASSEMBLED MASS MATRIX.
CC    AMM IS THE SEPERATED MASS MATRIX.
C+    ******************************************************************
      COMMON /B2/M(20,10)
      COMMON /B4/GMB(20,20)
      COMMON /B11/AMF,AV
      COMMON /B13/AF,AMP,FL
      COMMON /B14/AL
      COMMON /B15/RCWP,RCWF,AREA
      COMMON /B17/I,JJJ
      DIMENSION GME(20,20)
      DIMENSION   AA(10,10),ASM(20,20),BSM(20,20)
      REAL M
      ELMT=AL/FLOAT(I)
C     ******************************************************************
      P=((AMF+AMP)*ELMT)/420.0
      M(1,1)=156.*P
      M(1,2)=22.*ELMT*P
      M(1,3)=54.*P
      M(1,4)=-13.*ELMT*P
      M(2,2)=4.*(ELMT**2)*P
      M(2,3)=-M(1,4)
      M(2,4)=-3.*(ELMT**2)*P
      M(3,3)=M(1,1)
      M(3,4)=-M(1,2)
      M(4,4)=M(2,2)
      DO 1 II=1,4
      DO 1 JL=1,4
    1 M(JL,II)=M(II,JL)
      IF(I.NE.2.OR.JJJ.GE.3) GO TO 87
      PRINT 109
  109 FORMAT(/,5X,*MASS MATRIX IS*)
      PRINT 2,((M(II,JL),JL=1,4),II=1,4)
    2 FORMAT(2X,4E20.8)
   87 CONTINUE
C     ******************************************************************
      CALL ASMBL(M,GMB)
      CALL BNDRY(GMB,GMM)
      RETURN
      END


C     ******************************************************************
      SUBROUTINE DAMP
C     ******************************************************************
      REAL ELMT,AL,AMF,AV
C     C IS THE ELEMENTAL DAMPING MATRIX AMFAV.
CC    C1 IS THE ELEMENTAL DAMPING MATRIX DY/DT.
CC    C2 IS THE ELEMENTAL INTERNAL DAMPING MATRIX.
CC    C3 IS THE TOTAL ELEMENTAL DAMPING MATRIX.
CC    GCB IS THE ASSEMBLED DAMPING MATRIX.
C     GCM IS THE SEPERATED DAMPING MATRIX.
      COMMON/B5/C(10,10)
      COMMON/B6/GCM(20,20)
      COMMON/B11/AMF,AV
```

```
      COMMON /B12/AMI,E
      COMMON /B14/AL
      COMMON /B15/RCWF,AREA
      COMMON /B17/I,JJJ
      COMMON /B22/CBAR,CDASH
      COMMON /B23/C1(10,10)
      COMMON /B24/C2(10,10)
      COMMON /B25/CC,DI
      DIMENSION GCD(20,20)
      DIMENSION AA(10,10),ASM(20,20),BSM(20,20)
      DIMENSION C3(10,10)
      ELMT=AL/FLOAT(I)
C     ***************************************************************
      P=(AMF*AV)/3.
      C(1,1)=-36.*P
      C(1,2)=6.*ELMT*P
      C(1,3)=36.*P
      C(1,4)=-6.*ELMT*P
      C(2,1)=-6.*ELMT*P
      C(2,2)=4.*P
      C(2,3)=6.*ELMT*P
      C(2,4)=-(ELMT**2)*P
      C(3,1)=-36.*P
      C(3,2)=-6.*ELMT*P
      C(3,3)=36.*P
      C(3,4)=6.*ELMT*P
      C(4,1)=6.*ELMT*P
      C(4,2)=(ELMT**2)*P
      C(4,3)=-6.*ELMT*P
      C(4,4)=0.
      IF(I.NE.2.OR.JJJ.GE.3) GO TO 88
      PRINT 110
  110 FORMAT(/,5X,*FIRST DAMPING MATRIX IS*)
      PRINT30,((C(IK,JK),JK=1,4),IK=1,4)
   30 FORMAT(/,4X,4E20.8)
   88 CONTINUE
C     ***************************************************************
      PINKI=((RCWF*(DO/2.)*AV*CBAR)+CDASH)/420.0
      C1(1,1)=156.*ELMT*PINKI
      C1(1,2)=22.*(ELMT**2)*PINKI
      C1(1,3)=54.*ELMT*PINKI
      C1(1,4)=-13.*(ELMT**2)*PINKI
      C1(2,2)=4.*(ELMT**3)*PINKI
      C1(2,3)=-C1(1,4)
      C1(2,4)=-3.*(ELMT**3)*PINKI
      C1(3,3)=C1(1,1)
      C1(3,4)=-C1(1,2)
      C1(4,4)=C1(2,2)
C     ***********************************************
      DO 4 IK=1,4
      DO 4 JK=1,4
    4 C1(JK,IK)=C1(IK,JK)
      IF(I.NE.2.OR.JJJ.GE.3) GO TO 89
      PRINT 111
  111 FORMAT(/,5X,*SECOND DAMPING MATRIX IS*)
      PRINT31,((C1(IK,JK),JK=1,4),IK=1,4)
   31 FORMAT(/,4X,4E20.8)
   89 CONTINUE
C     ***************************************************************
      REAL ALPHA,MU,MI
      ALPHA=0.0
      MU=(SQRT(E*(AMP+AMF)/AMI))*ALPHA*(AL**2)
      PRINT1350,ALPHA,MU
 1350 FORMAT(5X,*ALPHA=*,E16.8,6X,*MU=*,E16.8)
      P=(MU*MI)/(ELMT**3)
      C2(1,1)=12.*P
      C2(1,2)=6.*ELMT*P
      C2(1,3)=-C2(1,1)
      C2(1,4)=C2(1,2)
      C2(2,2)=4.*(ELMT**2)*P
```

```
      C2(2,2)=-C2(1,2)
      C2(3,4)=2.*(ELMT**2)*P
      C2(3,3)=C2(1,1)
      C2(3,4)=-C2(1,2)
      C2(4,4)=C2(2,2)
      DO 1 IL=3,4
      DO 1 JL=3,4
    1 C2(JL,IL)=C2(IL,JL)
     +*********************************************************
      DO 7 IL=1,4
      DO 7 JL=1,4
      C3(IL,JL)=0.
      C3(IL,JL)=C3(IL,JL)+(C(IL,JL)+C1(IL,JL)+C2(IL,JL))
    7 CONTINUE
      IF(I.NE.2.OR.JJJ.GE.3) GO TO 90
      PRINT 112
  112 FORMAT(/,5X,*TOTAL DAMPING MATRIX IS*)
      PRINT 8,((C3(IL,JL),JL=1,4),IL=1,4)
    8 FORMAT(/,4X,4E20.8)
   90 CONTINUE
      CALL ASMBL(C3,GCB)
      CALL BNDRY(GCB,GCM)
      RETURN
      END

C     ***************************************************************
      SUBROUTINE ASMBL(AA,ASM)
C     ***************************************************************
CC    AA IS THE ELEMENTAL MATRIX.
C     ASM IS THE ASSEMBLED MATRIX.
      COMMON/B17/I,JJJ
      DIMENSION AA(10,10),ASM(20,20),BSM(20,20)
      N=2*(I+1)
      DO 1 II=1,N
      DO 1 JL=1,N
    1 ASM(II,JL)=0.0
      DO 2 K=1,I
      II=2*K-1
      JL=II
      II3=II+3
      JL3=JL+3
      DO 2 IK=II,II3
      DO 2 JK=JL,JL3
      L=IK-II+1
      LJ=JK-JL+1
    2 ASM(IK,JK)=ASM(IK,JK)+AA(L,LJ)
      IF(I.NE.2.OR.JJJ.GE.3) GO TO 79
      PRINT 103
  103 FORMAT(/,5X,*ASSEMBLED MATRIX AFTER B. C. IS*)
      PRINT104,((ASM(IK,JK),JK=1,N),IK=1,N)
  104 FORMAT(/,5X,6E15.8)
   79 CONTINUE
      RETURN
      END

C     ***************************************************************
      SUBROUTINE BNDRY(ASM,BSM)
C     ***************************************************************
CC    ASM IS THE ASSEMBLED MATRIX.
C     BSM IS THE SEPERATED MATRIX.
      COMMON/B17/I,JJJ
      DIMENSION ASM(20,20),BSM(20,20)
C     BOUNDARY CONDITIONS FOR PINNED-PINNED ROD.
      N=2*(I+1)
      N1=N-1
C     ROW OPERATION.
      DO 20 IK=1,N
      ASM(1,IK)=0.0
```

```
      ASM(N1,IK)=0.0
   20 CONTINUE
C     COLUMN OPERATION.
      DO 30 JK=1,N
      ASM(JK,1)=0.0
      ASM(JK,N1)=0.0
   30 CONTINUE
C     MAKING DIAGONAL ELEMENTS UNITY.
      ASM(1,1)=1.0
      ASM(N1,N1)=1.0
      IF(I.NE.2.OR.JJJ.GE.3) GO TO 78
      PRINT 106
  106 FORMAT(/,5X,*ASSEMBLED MATRIX AFTER B. C. IS*)
      PRINT50,((ASM(IK,JK),JK=1,N),IK=1,N)
   50 FORMAT(/,2X,6E15.8)
   78 CONTINUE
C     INTERCHANGING ROWS.
      DO 10 IK=2,N
      ASM(N1,IK)=ASM(N,IK)
   10 CONTINUE
C     INTERCHANGING COLUMNS.
      DO 40 JK=2,N
      ASM(JK,N1)=ASM(JK,N)
   40 CONTINUE
C     SEPERATING MATRIX BSM FROM MATRIX ASM.
      N=2*(I+1)
      N1=N-1
      IL=0
      DO 60 IK=2,N1
      IL=IL+1
      JL=0
      DO 60 JK=2,N1
      JL=JL+1
      BSM(IL,JL)=ASM(IK,JK)
   60 CONTINUE
      N=2*(I+1)
      N2=N-2
      IF(I.NE.2.OR.JJJ.GE.3) GO TO 80
      PRINT105
  105 FORMAT(/,5X,*SEPARATED MATRIX IS*)
      PRINT70,((BSM(IL,JL),JL=1,N2),IL=1,N2)
   70 FORMAT(/,4X,3E20.8)
   80 CONTINUE
      RETURN
      END

C     ***************************************************************
      SUBROUTINE MATMPY
C     ***************************************************************
CC    D IS THE UNITARY MATRIX.
CC    D1=INVERSE OF GSM*GMM.
CC    D2=INVERSE OF GSM*GCM.
C     DMM IS THE DYNAMICAL MATRIX.
      COMMON/B17/I,JJJ
      COMMON/B2/GSM(20,20)
      COMMON/B4/GMM(20,20)
      COMMON/B6/GCM(20,20)
      COMMON/B18/DMM(30,30)
      COMMON/B9/D(20,20)
      COMMON/B19/D1(20,20)
      COMMON/B8/D2(20,20)
C     FORMING UNITARY MATRIX D.
      N=(2*(I+1)-2)
      DO 8 IM=1,N
      DO 8 JM=1,N
      D(IM,JM)=0.0
      IF(IM.EQ.JM) D(IM,JM)=1.0
    8 CONTINUE
C     FORMING MATRIX D1.
```

```
      DO 1 II=1,N
      DO 1 JL=1,N
      D1(II,JL)=0.0
      DO 1 K=1,N
    1 D1(II,JL)=D1(II,JL)+(-GSM(II,K)*GMM(K,JL))
C     FORMING MATRIX D2.
      DO 2 IL=1,N
      DO 2 JL=1,N
      D2(IL,JL)=0.0
      DO 2 L=1,N
    2 D2(IL,JL)=D2(IL,JL)+(-GSM(IL,L)*GCM(L,JL))
C     FORMING DYNAMICAL MATRIX DMM.
      M=(2*(I+1)-2)
      NB=2*N
      DO 3 IK=1,NB
      DO 3 JK=1,NB
    3 DMM(IK,JK)=0.0
      L=N+1
      DO 4 IK=L,NB
      DO 4 JK=1,N
      II=IK-N
      JL=JK
    4 DMM(IK,JK)=DMM(IK,JK)+D1(II,JL)
      DO 5 IK=L,NB
      DO 5 JK=L,NB
      IL=IK-N
      JL=JK-N
    5 DMM(IK,JK)=DMM(IK,JK)+D2(IL,JL)
      DO 6 IK=1,N
      DO 6 JK=L,NB
      IM=IK
      JM=JK-N
    6 DMM(IK,JK)=DMM(IK,JK)+D(IM,JM)
      IF(I.NE.2.OR.JJJ.GE.3) GO TO 91
      PRINT 113
  113 FORMAT(/,5X,*DYNAMICAL MATRIX IS*)
      PRINT7,((DMM(IK,JK),JK=1,NB),IK=1,NB)
    7 FORMAT(/,4X,8E15.8)
   91 CONTINUE
      RETURN
      END
```